

1 Mapping the suitability of groundwater dependent 2 vegetation in a semi-arid Mediterranean area

3
4 Inês Gomes Marques¹; João Nascimento²; Rita M. Cardoso¹; Filipe Miguéns²; Maria
5 Teresa Condesso de Melo²; Pedro M. M. Soares¹; Célia M. Gouveia¹; Cathy Kurz
6 Besson¹

7
8 ¹ Instituto Dom Luiz; Faculty of Sciences, University of Lisbon, Campo Grande, Ed. C8, 1749-016,
9 Lisbon, Portugal

10 ² CERIS; Instituto Superior Técnico, University of Lisbon, 1049-001, Lisbon, Portugal

11
12 *Correspondence to:* Inês Gomes Marques (icgmarques@fc.ul.pt or icgmarques@isa.ulisboa.pt)

13 14 **Abstract**

15 Mapping the suitability of groundwater dependent vegetation in semi-arid Mediterranean areas is
16 fundamental for the sustainable management of groundwater resources and groundwater dependent
17 ecosystems (GDE) under the risks of climate change scenarios. For the present study the distribution of
18 deep-rooted woody species in southern Portugal was modeled using climatic, hydrological and
19 topographic environmental variables. To do so, *Quercus suber*, *Quercus ilex* and *Pinus pinea* were used
20 as proxy species to represent the Groundwater Dependent Vegetation (GDV). Model fitting was
21 performed between the proxy species Kernel density and the selected environmental predictors using 1) a
22 simple linear model and 2) a Geographically Weighted Regression (GWR), to account for auto-
23 correlation of the spatial data and residuals. When comparing the results of both models, the GWR
24 modelling results showed improved goodness of fitting, as opposed to the simple linear model. Climatic
25 indices were the main drivers of GDV density, followed with a much lower influence by groundwater
26 depth, drainage density and slope. Groundwater depth did not appear to be as pertinent in the model as
27 initially expected, accounting only for about 7% of the total variation against 88% for climate drivers

28 The relative proportion of model predictor coefficients was used as weighting factors for multicriteria
29 analysis, to create a suitability map to the GDV in southern Portugal showing where the vegetation most
30 likely relies on groundwater to cope with aridity. A validation of the resulting map was performed using
31 independent data of the Normalized Difference Water Index (NDWI) a satellite-derived vegetation index.
32 June, July and August of 2005 NDWI anomalies, to the years 1999-2009, were calculated to assess the
33 response of active woody species in the region after an extreme drought. The results from the NDWI
34 anomalies provided an overall good agreement with the suitability to host GDV. The model was
35 considered reliable to predict the distribution of the studied vegetation.

36 The methodology developed to map GDV's will allow to predict the evolution of the distribution of GDV
37 according to climate change and aid stakeholder decision-making concerning priority areas of water
38 resources management.

39

40 **Keywords:** Groundwater dependent vegetation, aridity, agroforestry, suitability map, Normalized
41 Difference Water Index

42

43

44 **1 Introduction**

45

46 Mediterranean forests, woodlands and shrublands, mostly growing under restricted water availability, are
47 one of the terrestrial biomes with higher volume of groundwater used by vegetation (Evaristo and
48 McDonnell, 2017). Future predictions of decreased precipitation (Giorgi and Lionello, 2008; Nadezhkina
49 et al., 2015), decreased runoff (Mourato et al., 2015) and aquifer recharge (Ertürk et al., 2014; Stigter et
50 al., 2014) in the Mediterranean region threaten the sustainability of groundwater reservoirs and the
51 corresponding dependent ecosystems. Therefore, a sustainable management of groundwater resources and
52 the Groundwater Dependent Ecosystems (GDE) is of crucial importance.

53 A widely used classification of GDE was proposed by Eamus et al. (2006). This classification
54 distinguishes three types: 1) Aquifer and cave ecosystems, which include all subterranean waters; 2)
55 Ecosystems reliant on emerging groundwater (e.g. estuarine systems, wetlands; riverine systems) and 3)
56 Ecosystems reliant on resident groundwater (e.g. systems where plants remain physiologically active
57 during extended drought periods, without a visible water source). Mapping GDE constitutes a first and
58 fundamental step to their active management. Several approaches have been proposed, from local field
59 surveys measuring plant transpiration of stable isotopes (Antunes et al. 2018) up to larger spatial scales
60 involving remote sensing techniques (e.g. Normalized Difference Vegetation Index – NDVI) (Barron et
61 al., 2014; Eamus et al., 2015; Howard and Merrifield, 2010), remote-sensing combined with ground-
62 based observations (Lv et al., 2013), geographic information system (GIS) (Pérez Hoyos et al., 2016a)
63 GIS combining field surveys (Condesso de Melo et al., 2015), or even statistical approaches (Pérez Hoyos
64 et al., 2016b).

65 Despite of a wide-ranging body of literature reviewing GDE's topics (Doody et al., 2017; Dresel et al.,
66 2010; Münch and Conrad, 2007), most of regional scale studies do not include Mediterranean regions.
67 Moreover, studies on ecosystems relying on resident groundwater frequently only focused on riparian
68 environments (Lowry and Loheide, 2010; O'Grady et al., 2006), with few examples in Mediterranean
69 areas (del Castillo et al., 2016; Fernandes, 2013; Hernández-Santana et al., 2008; Mendes et al., 2016).
70 There is a clear knowledge gap on the identification of phreatophyte species reliant on resident
71 groundwater and their associated vegetation (Robinson, 1958) in the Mediterranean region and the
72 management actions that should be taken to decrease the adverse effects of climate change.

73 In the driest regions of the Mediterranean basin, the persistent lack of water during the entire summer
74 periods gave an adaptive advantage to the vegetation that could either avoid or escape drought by
75 reaching deeper stored water up to the point of entirely relying on groundwater (Chaves et al., 2003;
76 Canadell et al., 1996; Miller et al., 2010). This drought-avoiding strategy is often associated to the
77 development of a dimorphic root system in woody species (Dinis 2014, David et al., 2013) or to hydraulic
78 lift and/or hydraulic redistribution mechanisms (Orellana et al., 2012). Those mechanisms provide the
79 ability to move water from deep soil layers, where water content is higher, to more shallow layers where
80 water content is lower (Horton and Hart, 1998; Neumann and Cardon, 2012). Hydraulic lift and
81 redistribution have been reported for several woody species of the Mediterranean basin (David et al.,

82 2007; Filella and Peñuelas, 2004) and noticeably for Cork oak (*Quercus suber* L.) (David et al., 2013;
83 Kurz-Besson et al., 2006; Mendes et al., 2016).

84 Mediterranean cork oak woodlands (Montados) are agro-silvo-pastoral systems considered as semi-
85 natural ecosystems of the southwest Mediterranean basin (Joffre et al., 1999) that have already been
86 referenced as a groundwater dependent terrestrial ecosystem (Mendes et al., 2016). Montados must be
87 continually maintained through human management by thinning, understory use through grazing,
88 ploughing and shrub clearing (Huntsinger and Bartolome, 1992) to maintain a good productivity,
89 biodiversity and ecosystems service (Bugalho et al., 2009). In the ecosystems of this geographical area,
90 the dominant tree species are the cork oak (*Quercus suber* L.) and the Portuguese holm oak (*Quercus ilex*
91 subs *rotundifolia* Lam.) (Pinto-Correia et al., 2011). Additionally, stone pine (*Pinus pinea* L.) has become
92 a commonly co-occurrent species in the last decades (Coelho and Campos, 2009). The use of groundwater
93 has been frequently reported for both *Pinus* (Antunes et al. 2018; Filella and Peñuelas, 2004; Grossiord et
94 al., 2016; Peñuelas and Filella, 2003) and *Quercus* genus (Barbeta and Peñuelas, 2017; David et al., 2007,
95 2013, Kurz-Besson et al., 2006, 2014; Otieno et al., 2006). Furthermore, the contribution of groundwater
96 to tree physiology has been shown to be of a greater magnitude for *Quercus* sp. as compared with *Pinus*
97 sp. (del Castillo et al., 2016; Evaristo and McDonnell, 2017).

98 *Q. suber* and *Q. ilex* have been associated with high resilience and adaptability to hydric and thermic
99 stress, and to recurrent droughts in the southern Mediterranean basin (Barbero et al., 1992). In Italy and
100 Portugal, during summer droughts *Q. ilex* used a mixture of rain-water and groundwater and was able to
101 take water from very dry soils (David et al., 2007; Valentini et al., 1992). An increasing contribution of
102 groundwater in the summer has also been shown for this species (Barbeta et al., 2015). Similarly, *Q.*
103 *suber* showed a seasonal shift in water sources, from shallow soil water in the spring to the beginning of
104 the dry period followed by a progressive higher use of deeper water sources throughout the drought
105 period (Otieno et al., 2006). In addition, the species roots are known to reach depths as deep as 13m in
106 southern Portugal (David et al., 2004). *P. pinea* has been recently included in the facultative phreatophyte
107 species (Antunes et al. 2018). This species shows a very similar root system (Montero et al., 2004) as
108 compared to cork oak (David et al., 2013), with large sinker roots reaching 5 m depth (Canadell et al.,
109 1996). Given the information available on water use strategies by the phreatophyte arboreous species of
110 the cork oak woodlands, *Q. ilex*, *Q. suber* and *P. pinea* were considered as proxies for arboreous
111 vegetation that belongs to GDE relying on resident groundwater (from here onwards designed as
112 Groundwater Dependent Vegetation – GDV).

113 GDV of the Mediterranean basin is often neglected in research. Indeed, still little is known about the
114 GDV distribution, but research has already been done on the effects of climate change in specific species
115 distribution, such as *Q. suber*, in the Mediterranean basin (Duque-Lazo et al., 2018; Paulo et al., 2015).
116 While the increase in atmospheric CO₂ and the rising temperature can boost tree growth (Barbeta and
117 Peñuelas, 2017; Bussotti et al., 2013; Sardans and Peñuelas, 2004), water stress can have a counteracting
118 effect on growth of both *Quercus ilex* (López et al., 1997; Sabaté et al., 2002) and *P. pinaster* (Kurz-
119 Besson et al., 2016). Therefore, it is of crucial importance to identify geographical areas where subsurface
120 GDV is present and characterize the environmental conditions this vegetation type is thriving in. This

121 would contribute to the understanding of how to manage these species under unfavorable future climatic
122 conditions.

123 The aim of this study was to address the mentioned gaps by creating a suitability map of the arboreous
124 phreatophyte species in southern Portugal, traducing their potential dependency on groundwater. We used
125 an integrated multidisciplinary methodology combining a geospatial modeling approach based on the
126 Geographically Weighted Regression (GWR) and a GIS multicriteria analysis approach, both relying on
127 forest inventory, edaphoclimatic conditions and topographic information. We expected this new
128 integrated procedure to grant a more reliable estimation of the vegetation dependency on groundwater
129 sources at the regional scale.

130 The Mapping methodology was based on the occurrence of known subsurface phreatophyte species and
131 well-known environmental conditions affecting water resources availability. Several environmental
132 predictors were selected according to their expected impact on water use and storage and then used in
133 GWR to model the density of *Q. suber*, *Q. ilex* and *P. pinea* occurrence in the Alentejo region (NUTSII)
134 of southern Portugal. To our knowledge, very few applications of GWR have been used to model species
135 distribution and only recently its use has spread in ecological research (Hu et al., 2017; Li et al., 2016;
136 Mazziotta et al., 2016). The coefficients obtained from the model equation for each predictor and
137 expressed as proportion of total sum of absolute coefficients were used as weights to build the suitability
138 map with GIS multi-factor analysis, after reclassifying each relevant environmental driver. The resulting
139 map was validated using the remote sensed vegetation index NDWI.

140 Based on former knowledge gathered from field surveys conducted in the region (Antunes et al. 2018,
141 Condesso de Melo et al., 2015, Kurz-Besson et al. 2006 & 2014, Otieno et al. 2006, David et al. 2013,
142 Pinto et al. 2013), on environmental conditions and the species ecophysiological needs, we hypothesized
143 that 1) groundwater depth together with climatic conditions play one of the most important environmental
144 roles in GDV's distribution and 2) groundwater depth between 1.5 and 15 m associated with xeric
145 conditions should favor a higher density of GDV and thus a larger use of groundwater by the vegetation.

146

147

148 **2 Material and Methods**

149

150 **2.1 Study area**

151 The administrative region of Alentejo (NUTSII) (fig01) covers an area of 31 604.9 km², between 37.22°
152 and 39.39° N in latitude and between 6.55° and 9.00° W in longitude. This study area is characterized by a
153 Mediterranean temperate mesothermic climate with hot and dry summers, defined as Csa in the Köppen
154 classification (APA, n.d.; ARH Alentejo, 2012a, 2012b). It is characterized by a sub-humid climate,
155 which has recently quickly drifted to semi-arid conditions (Ministério da Agricultura do Mar do
156 Ambiente e do Ordenamento do Território, 2013). A large proportion of the area (above 40%) is covered
157 by forestry systems (Autoridade Florestal Nacional and Ministério da Agricultura do Desenvolvimento
158 Rural e das Pescas, 2010) providing a high economical value to the region and the country (Sarmiento and
159 Dores, 2013).

160

161 **2.2 Kernel Density estimation of GDV**

162 Presence datasets of *Quercus suber*, *Quercus ilex* and *Pinus pinea* of the last Portuguese forest inventory
163 completed in 2010 (ICNF, 2013) were used to calculate Kernel density (commonly called heat map) as a
164 proxy for GDV suitability. The inventory registered the occurrence of each species on a 500m mesh grid
165 resolution, corresponding to a maximum occurrence of 4 counts per km². Only data points with one of the
166 three proxy species selected as primary and secondary occupation were used. The resulting Kernel density
167 was weighted according to tree cover percentage and was calculated using a quartic biweight distribution
168 shape, a search radius of 10 km, and an output resolution of 0.018 degrees, corresponding to a cell size of
169 1km. This variable was computed using QGIS version 2.14.12 (QGIS Development Team, 2017).

170

171

172 **2.3 Environmental variables**

173 Species distribution is mostly affected by limiting factors controlling ecophysiological responses,
174 disturbances and resources (Guisan and Thuiller, 2005). To characterize the study area in terms of GDV's
175 suitability, environmental variables expected to affect GDV's density were selected according to their
176 constraint on groundwater uptake and soil water storage. Within possible abiotic variables, landscape
177 topography, geology, groundwater availability and regional climate were considered. The twelve selected
178 variables for modeling purposes, retrieved from different data sources, are listed in Table 1. The software
179 used in spatial analysis was ArcGIS® software version 10.4.1 by Esri and R program software version
180 3.4.2 (R Development Core Team, 2016).

181

182 **2.3.1 Slope and soil characteristics**

183 The NASA and METI ASTER GDEM product was retrieved from the online Data Pool, courtesy of the
184 NASA Land Processes Distributed Active Archive Center (LP DAAC), USGS/Earth Resources
185 Observation and Science (EROS) Center, Sioux Falls, South
186 Dakota, https://lpdaac.usgs.gov/data_access/data_pool. Spatial Analyst Toolbox was used to calculate the
187 slope from the digital elevation model. Slope was used as proxy for the identification of shallow soil
188 water interaction with vegetation.

189 The map of soil type was obtained from the Portuguese National Information System for the Environment
190 - SNIAmb (© Agência Portuguesa do Ambiente, I.P., 2017) and uniformized to the World Reference
191 Base with the Harmonized World Soil Database v 1.2 (FAO et al., 2009). The vector map was converted
192 to raster using the Conversion Toolbox. To reduce the analysis complexity involving the several soil
193 types present in the map, soil types were regrouped in three classes, according to their capacity to store or
194 drain water (Table A1 in appendix A). The classification was based on the characteristics of each soil unit
195 (available water storage capacity, drainage and topsoil texture) from the Harmonized World Soil
196 Database v 1.2 (FAO et al., 2009). In the presence of dominant soil with low drainage capacity, a high
197 clay fraction in the top soil and a high available water content, lower scores were given in association to
198 decreased suitability for GDV by favoring non-GDV species. Otherwise, when soil characteristics
199 suggested water storage at deeper soil depths, lower water content, drainage and sandy topsoil texture,
200 higher scores were given.

201 Effective soil thickness (Table 1) was also considered for representing the maximum soil depth explored
202 by the vegetation roots. It constrains the expansion and growth of the root system, as well as the available
203 amount of water that can be absorbed by roots.

204

205 **2.3.2 Groundwater availability**

206 Root access to water resources is one of the most limiting factors for GDV's growth and survival,
207 especially during the dry season. The map of depth to water table was interpolated from piezometric
208 observations from the Portuguese National Information System on Water Resources (SNIRH) public data
209 base (<http://snirh.apambiente.pt>, last accessed on March 31st 2017) and the Study of Groundwater
210 Resources of Alentejo (ERHSA) (Chambel et al., 2007). Data points of large-diameter wells and
211 piezometers were retrieved for the Alentejo region (fig02) and sorted into undifferentiated, karst or
212 porous geological types to model groundwater depth. In the studied area, piezometers are exclusively
213 dedicated small diameter boreholes for piezometric observations, in areas with high abstraction volumes
214 for public water supply. Large diameter wells in this region are usually low yielding and mainly devoted
215 to private use and irrigation. Due to the large heterogeneity of geological media, groundwater depth was
216 calculated separately for each sub-basin. A total of 3158 data points corresponding to large wells and
217 piezometers were used, with uneven measurements between 1979 and 2017. For each piezometer an
218 average depth was calculated from the available observations and used as a single value. In areas with
219 undifferentiated geological type, piezometric level and elevation were highly correlated (>0.9), thus a
220 linear regression was applied to interpolate data. Ordinary kriging was preferred for the interpolation of

221 karst and porous aquifers, combining large wells and piezometric data points. The ordinary kriging was
222 calculated using a semi-variogram in which the sill, range and nugget were optimized to create the best fit
223 of the model to the data. To build a surface layer of the depth to water table, the interpolated surface of
224 the groundwater level was subtracted from the digital elevation model. Geostatistical Analyst ToolBox
225 was used for this task.

226 Drainage density is a measure of how well the basin is drained by stream channels. It is defined as the
227 total length of channels per unit area. Drainage density was calculated for a 10km grid size for the
228 Alentejo region, by the division of the 10km square area (A) in km² by the total stream length (L) in km,
229 as in Eq. (1).

$$230 \quad D = \frac{L}{A}, \quad (1)$$

231

232 **2.3.3 Regional Climate**

233 Temperature and precipitation datasets were obtained from the E-OBS
234 (<http://eca.knmi.nl/download/ensembles/ensembles.php>, last accessed on March 31st 2017) public
235 database (Haylock et al., 2008). Standardized Precipitation Evapotranspiration Index (SPEI), Aridity
236 Index (A_i) and Ombrothermic Indexes were computed from long-term (1951-2010) monthly temperature
237 and precipitation observations. The computation of potential evapotranspiration (PET) was performed
238 according to Thornthwaite (1948) and was calculated using the SPEI package (Beguería and Vicente-
239 Serrano, 2013) in R program.

240 SPEI multi-scalar drought index (Vicente-Serrano et al., 2010) was calculated over a 6 month interval to
241 characterize drought severity in the area of study using SPEI package (Beguería and Vicente-Serrano,
242 2013) for R program. SPEI is based on the normalization of the water balance calculated as the difference
243 between cumulative precipitation and PET for a given period at monthly intervals. Normalized values of
244 SPEI typically range between -3 and 3. Drought events were considered as severe when SPEI values were
245 between -1.5 and -1.99, and as extreme with values below -2 (Mckee et al., 1993). Severe and extreme
246 SPEI predictors were computed as the number of months with severe or extreme drought, counted along
247 the 60 years of the climate time-series.

248 While the SPEI index used in this study identifies geographical areas affected with more frequent extreme
249 droughts, the Aridity index distinguishes arid geographical areas prone to annual negative water balance
250 (with low A_i value) to more mesic areas showing positive annual water balance (with high A_i value). A_i
251 gives information related to evapotranspiration processes and rainfall deficit for potential vegetative
252 growth. It was calculated following Eq. (2) according to Middleton et al. (1992), where PET is the
253 average annual potential evapotranspiration and P is the average annual precipitation, both in mm for the
254 60 years period of the climate time-series. Dry lands are defined by their degree of aridity in 4 classes:
255 Hyperarid (A_i<0.05); Arid (0.05<A_i<0.2); Semi-arid (0.2<A_i<0.5) and Dry Subhumid (0.5<A_i<0.65)
256 (Middleton et al., 1992).

257
$$A_i = \frac{P}{PET}, \quad (2)$$

258 Ombrothermic Indexes were used to better characterize the bioclimatology of the study region (Rivas-
259 Martínez et al., 2011), by evaluating soil water availability for plants during the driest months of the year.
260 Four ombrothermic indexes were calculated according to a specific section of the year stated in Table 1,
261 and following Eq. (3), where P_p is the positive annual precipitation (accumulated monthly precipitation
262 when the average monthly mean temperature is higher than 0°C) and T_p is the positive annual
263 temperature (total in tenths of degrees centigrade of the average monthly temperatures higher than 0°).
264 Ombrothermic index presenting values below 2 for the analyzed months, can be considered as
265 Mediterranean bioclimatically. For non-Mediterranean areas, there is no dry period in which, for at least
266 two consecutive months, the precipitation is less than or equal to twice the temperature.

267
$$O = \frac{P_p}{T_p}, \quad (3)$$

268

269 **2.4 Selection of model predictors**

270 The full set of environmental variables was evaluated as potential predictors for the suitability of GDV
271 (based on the Kernel density of the proxy species). A preliminary selection was carried out, first by
272 computing Pearson's correlation coefficients between environmental variables and second by performing
273 a Principal Components Analysis (PCA) to detect multicollinearity. Covariates were discarded for
274 modeling according to a sequential procedure. Whenever pairs of variables presented a correlation value
275 above 0.4, the variable with the highest explained variance on the first axis of the PCA was selected. In
276 addition, selected variables had to show the lowest possible correlation values between them. Variables
277 showing low correlations and explaining a higher cumulative proportion of variability with the lowest
278 number of PCA axis were later selected as predictors for modeling. PCA was performed using the GeoDa
279 Software (Anselin et al., 2006) and Pearson's correlation coefficients were computed with Spatial Analyst
280 Tool .

281

282 **2.5 Model development**

283 When fitting a linear regression model based on the selected variables, the normal distribution and
284 stationarity of the response variable and residuals must be assured.

285 The Kernel density of the proxy GDV species, *Q. suber*, *Q. ilex* and *P. pinea*, showed a skewed normal
286 distribution. Therefore, a square-root transformation of the data was applied on the response variable,
287 before model fitting. To be able to compare the resulting model coefficients and use them as weighting
288 factors of the multi-criteria analysis to build the suitability map, the predictor variables were normalized
289 using the z-score function. This allows to create standardized scores for each variable, by subtracting the
290 mean of all data points from each individual data point, then dividing those points by the standard
291 deviation of all points, so that the mean of each z-predictor is zero and the deviation is 1.

292 Spatial autocorrelation and non-stationarity are common when using linear regression on spatial data. To
293 overcome these issues, the Geographically Weighted Regression (GWR) was used. This extension of the
294 Ordinary Least Squares (OLS) linear regression considers the spatial non stationarity in variable
295 relationships and allows the use of spatially varying coefficients while minimizing spatial autocorrelation
296 (Stewart Fotheringham et al., 1996). In this study, simple linear regression and GWR were both applied to
297 the dataset and their performances compared. Models were fitted on a 5% random subsample of the entire
298 dataset (reaching a total of 6214 selected data points), due to computational restrictions and to decrease
299 the spatial autocorrelation effect (Kühn, 2007). This methodology has already been applied with a
300 subsample of 10%, with points distant 10km from each other (Bertrand et al., 2016). In spite of the
301 subsampling, the minimum and maximum distance between two random data points were, respectively,
302 3.6 km and 16.7 km, providing a good representation of local heterogeneity, as shown in figures 05 and
303 06. An additional analysis showing an excellent agreement between the two datasets is presented in
304 FigA1 in appendix A.

305 Initially the model was constructed containing all selected predictors through the PCA and Pearson's
306 correlation analysis. Afterwards, predictors were sequentially discarded to ascertain the model presenting
307 lower second-order Akaike Information Criteria (AICc) and higher quasi-global R^2 chosen to predict the
308 suitability of GDV.

309 Adaptive Kernel bandwidths for the GWR model fitting were used due to the spatial irregularity of the
310 random subsample. Local search radius were obtained by minimizing the CrossValidation score (Bivand
311 et al., 2008) and thus minimizing the error of the local regressions. To analyze the performance of the
312 GWR model alone, the local and global adjusted R^2 were considered. To compare between the GWR
313 model and the simple linear model, the distribution of the model residuals was used to identify clustered
314 values as well as the AICc. The spatial autocorrelation of the models residuals was evaluated with the
315 Moran's I test (Moran, 1950) calculated from the Spatial Statistics Tool, and also graphically. GWR
316 model was fitted using the *spgwr* package from R program (Bivand and Yu, 2017).

317

318 **2.6 Suitability map building**

319 To create the suitability map all predictor layers included in the GWR model were classified, similarly to
320 Condesso de Melo et al. (2015) and Aksoy et al. (2017) . The likelihood of an interaction between the
321 vegetation and groundwater resources was scored from 1 to 3 for each predictor. Scores were assigned
322 after bibliographic review and expert opinion. The higher the score, the higher the likelihood, 1
323 corresponding to a weak likelihood and 3 indicating very high likelihood.

324 Groundwater depth was divided in two classes, according to the accessibility to shallow soil water above
325 1.5 m and the maximum rooting depth for Mediterranean woody species reaching 13 m, reported by
326 Canadell et al. (1996). Throughout the manuscript water between 0 and 1.5 m depth was designated as
327 shallow soil water, while water below 1.5 m depth was considered as groundwater. The depth class
328 between 0 and 1.5m was based on the riparian vegetation in semi-arid Mediterranean areas which is
329 mainly composed of shrub communities (Salinas et al., 2000) and presents a mean rooting depth of 1.5m

330 (Silva and Rego, 2004). The most common tree species rooting depth in riparian ecosystems is normally
 331 similar to the depth of fine sediment not reaching gravel substrates (Singer et al., 2012) and not reaching
 332 levels as deep as deep-rooted species. The minimum score was given to areas where groundwater depth
 333 was too shallow (below 1.5 m) considered to belong to emerging groundwater dependent vegetation.
 334 Areas with steep slope were considered to have superficial runoff and less recharge and influence
 335 negatively tree density (Costa et al., 2008). Those areas were treated as less suitable to GDV. Values of
 336 the Ombrothermic Index of the summer quarter and the immediately previous month (O_4) were split in 3
 337 classes according to Jenks natural breaks, with higher suitability corresponding to higher aridity. The
 338 higher values of A_i , corresponding to lower aridity had a score of 1, because a higher humid environment
 339 would decrease the necessity of the arboreous species to use deep water sources. Accordingly, an increase
 340 in aridity (lower values of A_i) has already been shown to increase tree decline (Waroux and Lambin,
 341 2012) and so lower A_i values corresponded to a score of 3, leaving the score 2 to intermediate values of
 342 A_i . Drainage density scoring was based on the drainage capability of the water through the
 343 hydrographical network of the river. A low drainage density (below 0.5) implies a high loss of water
 344 through runoff along the hydrographic network. This water lost for shallow soil horizons would be less
 345 available to the vegetation thus favoring a higher use of water from deep groundwater reservoirs
 346 (Rodrigues, 2011).

347 A direct compilation of the predictor layers could have been performed for the multicriteria analysis.
 348 However, some predictors might have a stronger influence on GDV's distribution and density than others.
 349 Therefore, there was a need to define weighting factors for each layer of the final GIS multicriteria
 350 analysis. Yet, due to the intricate relations between all environmental predictors and their effects on the
 351 GDV, experts and stakeholders suggested very different scoring for a same layer. Instead the relative
 352 proportion of each predictor was used locally, according to the GWR model (Eq. 4) as weighting factors.
 353 The final GIS multicriteria analysis was performed using the Spatial Analyst Tool by applying local
 354 model equations obtained for each of the 6214 coordinates of the Alentejo map (Eq.4),

$$355 \quad S_{GDV} = Intercept + coef_{p1} * [reclassified\ value\ X_1] + coef_{p2} * [reclassified\ value\ X_2] + coef_{p3} * \\ 356 \quad [reclassified\ value\ X_3] + \dots, \quad (4)$$

358 with S_{GDV} representing the suitability to Groundwater Dependent Vegetation, brackets representing the
 359 reclassified GIS X layer corresponding to the scoring and $coef_x$ indicating the relative proportion for the
 360 predictor x calculated as the ratio between the modulus of the local coefficient x and the sum of the
 361 modulus of all local coefficients..

362 According to this equation, lower values indicate a lower occurrence of groundwater use representing a
 363 lower GDV suitability while higher values correspond to a higher use of groundwater representing a
 364 higher GDV suitability. To allow for an easier interpretation, the data on suitability to GDV was
 365 subsequently classified based on their distribution value, according to Jenks natural breaks. This resulted
 366 in 5 suitability classes: "Very poor", "Poor", "Moderate", "Good" and "Very Good".

367

368 **2.7 Map evaluation**

369 Satellite derived remote-sensing products have been widely used to follow the impact of drought on land
370 cover and the vegetation dynamics (Aghakouchaket al. 2015). Vegetation indexes offer excellent tools to
371 assess and monitor plant changes and water stress (Asrar et al. 1989). The Normalized Difference Water
372 Index (NDWI) (Gao, 1996) is a satellite-derived index that aims to estimate fuel moisture content (Maki
373 et al., 2004) and leaf water content at canopy level, widely used for drought monitoring (Anderson et al.,
374 2010, Gu et al., 2007; Ceccato et al., 2002a). This index was chosen to be more sensitive to canopy water
375 content and a good proxy for water stress status in plants. Moreover, NDWI has been shown to be best
376 related to the greenness of Cork oak woodland's canopy, expressed by the fraction of intercepted
377 photosynthetically active radiation (Cerasoli et al., 2016).

378 In order to validate the GDV suitability map obtained in our study, we calculated anomalies of the
379 Normalized Difference Water Index (NDWI) (Gao, 1996) between an extreme dry year (2005) and the
380 median value of the surrounding 10 year period (1999-2009). NDWI is computed using the near infrared
381 (NIR) and the short-wave infrared (SWIR) reflectance, which makes it sensitive to changes in liquid
382 water content and in vegetation canopies (Gao, 1996; Ceccato et al., 2002a, b). The index computation
383 (Eq. 5) was further adapted by Gond et al. (2004) to SPOT-VEGETATION instrument datasets, using
384 NIR (0.84 μm) and MIR (1.64 μm) channels, as described by Hagolle et al. (2005).

$$385 \quad NDWI = \frac{\rho_{NIR} - \rho_{MIR}}{\rho_{NIR} + \rho_{MIR}}. \quad (5)$$

386 Following Eq. (5), NDWI data was computed using B3 and MIR data acquired from VEGETATION
387 instrument on board of SPOT4 and SPOT5 satellites. Extraction and corrections procedures applied to
388 optimize NDWI series are fully described in Gouveia et al. (2012).

389 The NDWI anomaly was computed as the difference between NDWI observed in June, July and August
390 of 2005 and the median NDWI for the considered month for the period 1999 to 2009. June was selected
391 to provide the best signal from a still fully active canopy of woody species while the herbaceous layer had
392 usually already finished its annual cycle and dried out. The hydrological year of 2004/2005 was
393 characterized by an extreme drought event over the Iberian Peninsula, where less than 40% of the normal
394 precipitation was registered in the southern area (Gouveia et al., 2009). Thus, in June 2005 the vegetation
395 of the Alentejo region was already coping with an extreme long-term drought, which was well captured
396 by the anomaly of the NDWI index (negative values), as formerly shown by Gouveia et al. 2012.

397

398 **2.8 Sensitivity analysis**

399 Sensitivity analyses are conducted to identify model inputs that cause significant impact and/or
400 uncertainty in the output. They can be used to identify key variables that should be the focus of attention
401 to increase mode robustness in future research or to remove redundant inputs from the model equation
402 because they do not have significant impact on the model output. Based on bootstrapping simulations
403 (Tian et al., 2014), a sensitivity analysis was conducted on the GWR model by perturbing one input

404 predictor at time while keeping the rest of the equation unperturbed. To simulate perturbations, 10000
405 values were randomly selected within the natural range of each input variable observed in the Alentejo
406 region. Those random values were then used to run 10000 simulations of the local equation of the GWR
407 model for each of the 6214 coordinates of the geographical area. Local outputs corresponding to the
408 predicted GDV density were then calculated for each perturbed input variable (A_i , O_4 , W , D and s). The
409 range of output values was calculated to reflect the sensibility of the model for the perturbed input
410 variable. The overall sensibility of the model to all input variables was estimated as the absolute
411 difference between the minimum output value and the sum of maximum output values of all predictors,
412 thus representing the maximum possible output range observed after perturbing all predictors.

413

414

415

416 **3 Results**

417

418 **3.1 Kernel Density**

419 Within the studied region of Portugal, the phreatophyte species *Quercus suber*, *Quercus ilex* and *Pinus*
420 *pinea* were not distributed uniformly throughout the territory. Areas with higher Kernel density (or higher
421 distribution likelihood) were mostly spread between the northern part of Alentejo region and the western
422 part close to the coast, with values ranging between 900 and 1200 occurrences in 10 km search radius
423 (fig03). Two clusters of high density also appeared below the Tagus river. The remaining study area
424 presented mean density values, with very low densities in the area of the river Tagus and in the center
425 south.

426

427 **3.2 Environmental conditions**

428 The exploratory analysis of the variables performed through the PCA and the Pearson's correlation matrix
429 confirmed the presence of multicollinearity. From the initial variables (Table 1), Thickness (T), number
430 of months with severe and extreme SPEI (respectively, SPEI_s and SPEI_e), Annual Ombrothermic Index
431 (O), Ombrothermic Index of the hottest month of the summer quarter(O₁) and Ombrothermic Index of the
432 summer quarter (O₃) were discarded, while the variables slope (s), drainage density (D), soil type (S_t),
433 groundwater depth (W), A_i and O₄ were maintained for analysis (figA2 and Table A2 in appendix). A
434 sequential removal of one predictor from the initial modeling including six variables was performed
435 (Table 2), after which the model was reduced to 5 variables. Therefore, out of the initial 12 variables
436 considered (fig04) to explain the variation of the Kernel density of GDV in Alentejo, the following
437 variables were endorsed: A_i, O₄, W, D and s.

438 In most part of the Alentejo region, slope was below 10% (fig04e) and coastal areas presented the lowest
439 values and variability. Highest values of groundwater depth (fig04c), reaching a maximum of 255 m,
440 were found in the Atlantic margin of the study area, mainly in Tagus and Sado river basins. Several other
441 small and confined areas in Alentejo also showed high values, corresponding to aquifers of porous or
442 karst geological types. Most of the remaining study area showed groundwater depths ranging between 1.5
443 m and 15 m. Figures 04a and 04b indicate the southeast of Alentejo as the driest area, given by minimum
444 values of A_i (0.618), and much higher potential evapotranspiration than precipitation. Besides, O₄
445 presented a maximum value (1.166) for this region (meaning that soil water availability was not
446 compensated by the precipitation of the previous M-J-J-A months). This is also supported by the higher
447 drainage density in the southeast which indicates a lower prevalence of shallow soil water due to higher
448 stream length by area.

449 Combining all variables, it was possible to distinguish two sub-regions with distinct conditions: the
450 southeast of Alentejo and the Atlantic margin. The latter is mainly distinguished by its low slope areas,
451 shallower groundwater and more humid climatic conditions than the southeast of Alentejo.

452

453 3.3 Regression models

454 The best model to describe the GDV distribution was found through a sequential discard of each variable
455 (Table 2) and corresponded to the model with a distinct lower AICc (18050.76) than the second lowest
456 AICc (27389.74) and showed an important increase in quasi-global R^2 (from 0.926 for the second best
457 model to 0.992 for the best one). The best model fit was obtained with A_i , O_4 , W , D and s . This final
458 model was then applied to the GIS layers to map the suitability of GDV in Alentejo, according to Eq. 6.

$$459 S_{GDV} = Intercept + A_i \text{ coef}_p * [\text{reclassified } A_i \text{ value}] + O_4 \text{ coef}_p * [\text{reclassified } O_4 \text{ value}] + W \text{ coef}_p * \\ 460 [\text{reclassified } W \text{ value}] + D \text{ coef}_p * [\text{reclassified } D \text{ value}] + s \text{ coef}_p * [\text{reclassified } s \text{ value}],$$

461 (6)

462 Local adjusted R^2 of the GWR model was highly variable throughout the study area, ranging from 0 to
463 0.99 (fig05), however the local R^2 values below 0.5 corresponded to only 0.3% of the data. The lower R^2
464 values were distributed throughout the Alentejo area, with no distinct pattern. The overall fit of the GWR
465 model was high (Table 3). The adjusted regression coefficient indicated that 99% of the variation in the
466 data was explained by the GWR model, while only 2% was explained by the simple linear model (Table
467 3). Accordingly, GWR had a substantially lower AICc when compared with the simple linear model,
468 indicating a much better fit.

469 The spatial autocorrelation given by the Moran Index (Griffith, 2009; Moran 1950) retrieved from the
470 geospatial distribution of residual values was significant for both the GWR and the linear models,
471 indicating that observations are geospatially dependent on each other to a certain level. However, this
472 dependence was substantially lower for the GWR model than for the linear model (z-score of 50.24 and
473 147.56 respectively). In the GWR model (fig06a) the positive and negative residual values were much
474 more randomly scattered throughout the study region than in the linear model (fig06b), highlighting a
475 much better performance of the GWR, which minimized residual autocorrelation. Indeed, in the linear
476 model (fig06b), positive residuals were condensed in the right side of Tagus and Sado river basins, while
477 negative values were mainly present on the left side of the Tagus river and in the center-south of Alentejo.

478 The spatial distribution of the coefficients of GWR predictors is presented in Fig07. They were later used
479 for the computation of the GDV suitability score for each data point (Eq.6). The coefficient variability
480 was three times higher for the A_i as compared to O_4 (fig08a), reaching 66% and 22% respectively. For W ,
481 D and s , the coefficient variation was much lower, representing only about 6.2%, 3.8% and 1.2% of the
482 total variation observed in the coefficients, respectively. The remaining variables showed a median close
483 to 0 and the O_4 was the second with higher variability followed by the W . The coefficient median values
484 were, respectively, -3.40, 0.29, -0.015, -0.018 and 0.022 for A_i , O_4 , W , D and s variables.

485 The distributions of negative coefficients were similar for A_i and the O_4 variables (fig07a and fig07b),
486 with lower values in the southern coastal area, and in the Tagus river watershed. The highest absolute
487 values were mostly found for A_i in the southern area of the Alentejo region and on smaller patches in the
488 northern region. In the center and eastern areas of Alentejo, a higher weight of the groundwater depth

489 coefficient could be found (fig07c), approximately matching a higher influence of slope (fig07e). The
490 groundwater depth seemed to have almost no influence on GDV density in the Tagus river watershed,
491 expressed by coefficients mostly null around the riverbed (fig07c). The coefficient distribution of D and
492 O_4 shows some similarities, mostly in the center and southeast of Alentejo (fig07d). Extreme values of O_4
493 coefficients were mostly concentrated in the eastern part of the Tagus watershed and in the southern
494 coastal area included in the Sado watershed. Slope coefficient values showed the lowest amplitude
495 throughout the study area (fig07e), with prevailing high positive values gathered mainly in the center of
496 the study area and in the Tagus river watershed (northwest of the study center).

497

498 **3.4 GDV Suitability map**

499 The classification of the 5 endorsed environmental predictors is presented in Table 4 and their respective
500 maps in figure B1 in appendix B. Rivers Tagus and Sado had an overall large impact on GDV's
501 suitability for each predictor, with the exception of W. This is due to a higher water availability reflected
502 by the values of O_4 , D and lower slopes due to the alluvial plains of the Tagus river (figs. B1b, d and e in
503 appendix B). Moreover, those regions presented higher humidity conditions (through analysis of the A_i in
504 fig B1a in appendix B) and groundwater depths outside the optimum range (Fig. B1c in appendix B),
505 therefore less suitable for GDV. Optimal conditions for groundwater access were mainly gathered in the
506 interior of the study region (fig. B1c in appendix B), with the exception of some confined aquifers in the
507 northeast and southeast of the study region. Favorable slopes for GDV were mostly highlighted in the
508 Tagus river basin area, where a good likelihood of interaction between GDV and groundwater could be
509 identified (fig. B1e in appendix B).

510 The final map illustrating the suitability to GDV is shown in Fig. 09. The largest classified area (8
511 787km²) presented a very poor suitability to GDV, corresponding to approximately a quarter of the total
512 study area (29%). This percentage was followed closely by the moderate suitability to GDV which
513 occupied 26% (8000km²). Overall, the two less suitable classes (very poor and poor) represented 47% of
514 the study area, whilst the two best ones and the moderate class (very good, good and moderate)
515 represented 53%. Consequently, most of the study area showed moderate to high suitability to GDV. The
516 very good and good suitability classes cover an arch from the most south and northeastern area of the
517 Alentejo region, passing through the Sado and southern Guadiana river basins and close to the coastal line
518 at 38°N. Most of the center of the study area showed moderate to very good suitability to GDV, while the
519 areas corresponding to the alluvial deposits of the Tagus river showed poor to very poor suitability.

520 The suitability to GDV in the Alentejo region was mainly driven by A_i , given that the highest coefficient
521 variability was associated to the A_i predictor in the GWR model equation. Consequently a similar
522 distribution pattern can be observed between the suitability map and the aridity index predictor (fig04a
523 and fig09). Areas with good or very good suitability mostly matched areas of A_i with score 3,
524 corresponding to aridity index values above 0.75 (Fig. B1a in appendix B). On the other hand, the lowest
525 suitability classes showed a good agreement with the lowest scores given to W (fig. B1c in appendix B),
526 mostly in the coastal area and in the Tagus river basin.

527

528 **3.5 Map evaluation**

529 To evaluate the suitability map developed in the present study, the results were compared with the NDWI
530 anomaly considering the month of June of the dry year of 2005 in the Alentejo area (fig10). Both maps
531 (figs 09 and 10) showed similar patterns, with higher presence of GDV satisfactorily matching areas with
532 the lowest NDWI anomaly. From June to September in an extremely dry year, non-DGV plants can be
533 expected to experience a severe drought stress as in any regular summer period. Thus, those plants should
534 show almost zero anomaly. By opposition, GDV plants coping well with usual summer drought can be
535 expected to suffer an unusual stress under an extreme dry year even having access to groundwater (Kurz-
536 Besson et al. 2006 & 2014, Otieno et al. 2006, David et al. 2013), with a negative impact of groundwater
537 drawdown (Antunes et al., 2018). Therefore, GDV plants should show negative NDWI anomalies.

538 The NDWI anomaly was mostly negative over the Alentejo territory indicating a lower leaf water content
539 in June and July 2005 than usual. The loss of water attributed to the extreme drought was mostly
540 matching geographical areas with the highest GDV suitability (fig09). Water loss was less pronounced in
541 the central area of the Alentejo region between the Guadiana and Sado river basins, where the vegetation
542 is less dense (fig03). Areas with null NDWI anomaly values (indicating no NDWI change) were mostly
543 distributed on the coastal area of the Atlantic ocean or close to riverbeds, namely in the Tagus and Sado
544 floodplains, matching areas of very poor suitability for GDV in Figure 09.

545 Despite an overall good agreement, the adequation between the density, suitability and NDWI maps was
546 not perfect. Indeed, some patches showing a high vegetation occurrence/density and large NDWI
547 anomalies also matched an area of very poor suitability for GDV.

548

549 **3.6 Sensitivity analysis**

550 The sensitivity of the model in response to the perturbation of each one of the input variables (A_i , O_4 , W ,
551 D and s) is presented on Figures 11a to 11e. The overall sensitivity of the model is further presented on
552 Figure 11f. For any input variable, the model sensitivity (fig11a to 11e) was higher where absolute values
553 of local coefficients were also higher (fig07a to 07e). The maximum impact on GDV's density,
554 corresponding to the maximum output range observed after perturbation (fig08b), was observed when
555 perturbing the A_i , accounting for 66% of the total variability. The second highest impact was observed
556 after perturbing the O_4 , corresponding to 22%. The variability in the model outputs observed after
557 perturbing the remaining variables W , D and s accounted for 7%, 4% and 1% of the total accumulated
558 variability, respectively (fig08b). The highest variability in the GWR model output was mostly observed
559 in the central part of the southern half of the Alentejo region, as well as close to the main channels of the
560 Guadiana and Tagus rivers (fig11f). Furthermore, areas with higher model sensitivity (fig11f)
561 significantly matched higher model performance expressed by R^2 (fig05), assessed with a Kruskal-Wallis
562 test ($p < 0.0001$ ***).

563

564 4 Discussion

565

566 4.1 Modeling approach

567 The Geographically Weighted Regression model has been used before in ecological studies (Li et al.,
568 2016; Mazziotta et al., 2016), but never for the mapping of GDV, to our knowledge. This approach
569 considerably improved the goodness of fit when compared to the linear model, with a coefficient of
570 regression (R^2) increasing from 0.02 to 0.99 at the global level, and an obvious reduction of residual
571 clustering. Despite those improvements, it has not been possible to completely eliminate the residual
572 autocorrelation after fitting the GWR model.

573 Kernel density for the study area provided a strong indication of presence and abundance of the tree
574 species considered as GDV proxy for modeling. The Mediterranean cork woodlands dominate about 76%
575 of the Alentejo region (while only 7% is covered by stone pine). In those systems, tree density is known
576 to be a tradeoff between climate drivers (Joffre 1999, Gouveia & Freitas 2008) and the need for space for
577 pasture or cereal cultivation in the understory (Acácio & Holmgreen 2014). In our study, the
578 anthropologic management of agroforestry systems in the Alentejo region has not been taken into
579 account. According to a recent study of Cabon et al. (2018) where thinning played an important role in *Q.*
580 *ilex* density in a Mediterranean climate site, anthropologic management could, at least partially, explain
581 the non-randomness of the residual distribution after GWR model fitting as well as the mismatches
582 between the GDV and the NDWI evaluation maps.

583 Another explanation of the reminiscent autocorrelation after GWR fitting could be the lack of
584 groundwater dependent species in the model. For example, *Pinus pinaster* Aiton was excluded due to its
585 more humid distribution in Portugal, and due to conflicting conclusions driven from previous studies to
586 pinpoint the species as a potential groundwater user (Bourke, 2004; Kurz-Besson et al., 2016). In
587 addition, olive trees were also excluded although the use of groundwater by an olive orchard has been
588 recently proved (Ferreira et al., 2018), however with a weak contribution of groundwater to the daily root
589 flow, and thus with no significant impact of groundwater on the species physiological conditions.

590 Methods previously used by Doody et al., (2017) and Condesso de Melo et al. (2015) to map specific
591 vegetation relied solely on expert opinion, e.g. Delphi panel, to define weighting factors of environmental
592 information for GIS multicriteria analysis. In our study, the GWR modelling approach was used to assess
593 weighting factors for each environmental predictor in the study area, to build a suitability map for the
594 GDV in southern Portugal. This allowed an empirical determination of the local relevance of each
595 environmental predictor in GDV distribution, thus avoiding the inevitable subjectivity of Delphi panels.

596 Also, by combining the GWR and GIS approaches we believe the final suitability map provides a more
597 reliable indication of the higher likelihood for groundwater dependency and a safer appraisal of the
598 relative contribution of groundwater by facultative deep-rooted phreatophytes species in the Alentejo
599 region.

600

601 Modelling of the entire study area at a regional level did not provide satisfactory results. Therefore, we
602 developed a general model varying locally according to local predictor coefficients. The local influence of
603 each predictor was highly variable throughout the study area, especially for climatic predictors reflecting
604 water availability and stress conditions. The application of the GWR model did not only allow for a
605 localized approach, by decreasing the residual error and autocorrelation over the entire studied region, but
606 also provided insights on how GDV's density can be explained by the main environmental drivers locally.

607 The GWR model appeared to be highly sensitive to coefficient fitting corresponding to a good model fit,
608 as expected in a spatially varying model. As so, high coefficients are highly reliable in the GWR model in
609 our study. Yet, the high spatial variability of local coefficients might reflect a weak physical meaning of
610 the GWR model that challenges its direct application in other regions, even under similar climate
611 conditions. Predictor coefficients showed a similar behavior in the spatial distribution of the coefficients.
612 This was noticeable for the aridity index and the groundwater depth in the Tagus and Sado river basins.
613 Groundwater depth had no influence on GDV's density in these areas and similarly, the coefficient of
614 aridity index showed a negative effect of increased humidity on GDV's density. In addition, a cluster of
615 low drainage density values matched these areas. Due to the lower variability and impact of the drainage
616 density and slope on the GDV's density, these variables might not impact significantly this vegetation
617 density in future climatic scenarios.

618

619 **4.2 Suitability to Groundwater Dependent Vegetation**

620 According to our results, more than half of the study area appeared suitable for GDV. However, one
621 quarter of the studied area showed lower suitability to GDV. The lower suitability to this vegetation in the
622 more northern and western part of the studied area included the coastal area and the Tagus river basin.
623 Those are the moist humid areas of the study area, where GDV is unlikely to rely on groundwater during
624 the drought season because rainfall water stored in shallow soil horizons is mostly available.

625 The proxy species (Cork oak, Holm oak and Stone pine) can perfectly grow under sub-humid
626 Mediterranean climate conditions, without relying as much on groundwater to survive as in more xeric
627 semi-arid areas (Abad Vinas et al., 2016). As facultative phreatophyte species, their presence/abundance
628 is only an indication of a possible use of groundwater. The study provided by Pinto et al. (2013) have
629 shown that Cork oak, for example, can perfectly thrive were very shallow groundwater is available while
630 suffering drought stress were groundwater source is lower but still extracted by trees. Also, former studies
631 have shown that in the extreme dry year of 2005, Cork oak experienced a severe drought stress, close to
632 the cavitation threshold, although its main water source was groundwater (David et al. 2013, Kurz-Besson
633 et al. 2006, 2014). These findings can explain that part of the maximum density (Fig. 04) matches the area
634 of very poor suitability for GDV (Fig. 09). Elsewhere, the better agreement between the two maps reflects
635 the dominance of the aridity index on the vegetation's occurrence. Groundwater depth appeared to have a
636 lower influence on GDV density than climate drivers, as reflected by the relative low magnitude of the W
637 coefficient and outputs of our model outcomes. This surprisingly disagrees with our initial hypothesis
638 because groundwater represents a notable proportion of the transpired water of deep-rooting

639 phreatophytes, reaching up to 86% of absorbed water during drought periods and representing about
640 30.5% of the annual water absorbed by trees (David et al. 2013, Kurz-Besson et al. 2014). Nonetheless,
641 this disagreement should be regarded cautiously due to the poor quality of piezometric data used and the
642 complexity required for modelling the water table depths. Besides, the linear relationship between water
643 depth and topography applied to areas of undifferentiated geological type can be weakened by a complex
644 non-linear interaction between topography, aridity and subsurface conductivity (Condon and Maxell,
645 2015). Moreover, the high variability in geological media, topography and vegetation cover at the
646 regional scale did not allow to account for small changes in groundwater depth (<15 m deep), which has a
647 huge impact on GDV suitability (Canadell et al., 1996; Stone and Kalisz, 1991). Indeed, a high spatial
648 resolution of hydrological database is essential to rigorously characterize the spatial dynamics of
649 groundwater depth between hydrographic basins (Lorenzo-Lacruz et al., 2017). Unfortunately, such
650 resolution was not available for our study area.

651 The aridity and ombrothermic indexes were the most important predictors of GDV density in the Alentejo
652 region, according to our model outcomes. Our results agree with previous findings linking tree cover
653 density and rooting depth to climate drivers such as aridity, at a global scale (Zomer et al., 2009; Schenk
654 and Jackson, 2002) and specifically for the Mediterranean oak woodland (Gouveia and Freitas 2008,
655 Joffre et al. 1999). Through previous studies showing the similarities in vegetation strategies to cope with
656 water scarcity in the Mediterranean basin (Vicente-Serrano et al., 2013) or the relationship between
657 rooting depth and water table depth increased with aridity at a global scale (Fan et al., 2017) we can admit
658 that the most relevant climate drivers pinpointed here are similarly important to map GDV in other semi-
659 arid regions. In this study, the most important environmental variables that define GDV's density in a
660 semi-arid region were identified, helping to fill the gap of knowledge for modelling this type of
661 vegetation. However, the coefficients to be applied when modelling each variable need to be calculated
662 locally, due to their high spatial variability.

663 Temporal piezometric data would further help discriminate areas of optimal suitability to GDV, either
664 during the wet and the dry seasons, because the seasonal trends in groundwater depth are essential under
665 Mediterranean conditions. Investigations efforts should be invested to fill the gap either by improving the
666 Portuguese piezometric monitoring network, or by assimilating observations with remote sensing
667 products focused on soil moisture or groundwater monitoring. This has already been performed for large
668 regional scale such as GRACE satellite surveys, based on changes of Earth's gravitational field. So far,
669 these technologies are not applicable to Portugal's scale, since the coarse spatial resolution of GRACE
670 data only allows the monitoring of large reservoirs (Xiao et al. 2015).

671

672 **4.3 Validation of the results**

673 The understory of woodlands and the herbaceous layer of grasslands areas in southern Portugal usually
674 ends their annual life cycles in June (Paço et al. 2009), while the canopy of woody species is still fully
675 active with maximum transpiration rates and photosynthetic activities (Kurz-Besson et al. 2014, David et

676 al. 2007, Awada et al. 2003). This is an ideal period of the year to spot differential response of the canopy
677 of woody species to extreme droughts events using satellite derived vegetation indexes (Gouveia 2012).

678 The spatial patterns of NDWI anomaly in June 2005 seem to indicate that the woody canopy showed a
679 strong loss of canopy water in the areas where tree density and GDV suitability were higher (figs 03, 09 and
680 10). This occurred although trees minimized the loss of water in leaves with a strong stomatal limitation
681 in response to drought (Kurz-Besson et al. 2014, Grant et al. 2010). In the most arid area of the region
682 where Holm oak is dominant but tree density is much lower, the NDWI anomaly was generally less
683 negative thus showing a lower water stress or higher canopy water content. Holm oak (*Quercus ilex* spp
684 *rotundifolia*) is well known to be the most resilient species to dry and hot conditions in Portugal, due to
685 its capacity to use groundwater, associated to a higher water use efficiency (David et al. 2007).

686 Furthermore, the dynamics of NDWI anomaly over the summer period (fig 10a, b and c) pointed out that
687 the lower water stress status on the map is progressively spreading from the most arid areas to the milder
688 ones from June to August 2005, despite the intensification of drought conditions. This endorses the idea
689 that trees manage to cope with drought by relying on deeper water sources in response to drought,
690 replenishing leaf water content despite the progression and intensification of drought conditions. Former
691 studies support this statement by showing that groundwater uptake and hydraulic lift were progressively
692 taking place after the onset of drought by promoting the formation of new roots reaching deeper soil
693 layers and water sources, typically from July onwards, for cork oak in the Alentejo region (Kurz-Besson
694 et al., 2006, 2014). Root elongation following a declining water table has also been reported in a review
695 on the effect of groundwater fluctuations on phreatophyte vegetation (Naumburg et al. 2005).

696 Our results and the dynamics of NDWI over summer 2005 tend to corroborate the studies of Schenk and
697 Jackson (2002) and Fan et al. (2017), by suggesting a larger/longer dependency of GDV on groundwater
698 with higher aridity. Further investigation needs to be carried on across aridity gradients in Portugal and
699 the Iberian Peninsula to fully validate this statement, though.

700 Overall, the map of suitability to GDV showed a good agreement with the NDWI validation maps. The
701 main areas showing good GDV suitability and highest NDWI anomalies are mostly matching in both
702 maps. The good agreement between our GDV suitability maps, and NDWI dynamic maps opens the
703 possibility to apply and extend the methodology to larger geographical areas such as the Iberian Peninsula
704 and to the simulation of the impact of climate changes on the distribution of groundwater dependent
705 species in the Mediterranean basin.

706 Simulations of future climate conditions based on RCP4.5 and RCP8.5 emission scenarios (Soares et al.,
707 2015, 2017) predict a significant decrease of precipitation for the Guadiana basin and overall decrease for
708 the southern region of Portugal within 2100. Agroforestry systems relying on groundwater resources,
709 such as cork oak woodlands, may show a decrease in productivity and ecosystem services or even face
710 sustainability failure. Many studies carried out on oak woodlands in Italy and Spain identified drought as
711 the main driving factor of tree die-back and as the main climate warning threatening oak stands
712 sustainability in the Mediterranean basin (Gentilesca et al. 2017). An increase in aridity and drought
713 frequency for the Mediterranean (Spinoni et al., 2017) will most probably induce a geographical shift of
714 GDV vegetation toward milder/wetter climates (Lloret et al., 2004; Gonzalez P., 2001).

715

716 **4.4 Key limitations**

717 The GWR modelling approach used to estimate weighting factors is mostly stochastic. Consequently, the
718 large spatial variability and symmetrical fluctuations around zero (Fig 08b) denote a weak physical
719 meaning of the estimated coefficients, at least at the resolution chosen for the study. Also, the local nature
720 of the regression coefficients makes the model difficult to directly apply in other regions, even with
721 similar climate conditions, unless the methodology is properly fitted to local conditions/predictors.

722 With the methodology applied in this study, weighting factors can be easily evaluated solely from local
723 and regional observations of the studied area. Nonetheless, the computation of model coefficients or
724 expert opinion to assess weighting factors, require recurrent amendments, associated with updated
725 environmental data, species distribution and revised expert knowledge (Doody et al., 2017).

726 The evolution of groundwater depth in response to climate change is difficult to model on a large scale
727 based on piezometric observations because it requires an excellent knowledge of the components and
728 dynamics of water catchments. Therefore, a reliable estimation of the impact of climate change on GDV
729 suitability in southern Portugal could only been performed on small scale studies. However, the GWR
730 model appeared to be much more sensitive to climate drivers than the other predictors, given that 88% of
731 the model outputs variability was covered by climate indexes A_i and O_4 . Nevertheless, changes in climate
732 conditions only represent part of the water resources shortage issue in the future. Global-scale changes in
733 human populations and economic progresses also rule water demand and supply, especially in arid and
734 semi-arid regions (Vörösmarty et al., 2000). A decrease in useful water resources for human supply can
735 induce an even higher pressure on groundwater resources (Döll, 2009), aggravating the water table
736 drawdown caused by climate change (Ertürk et al., 2014). Therefore, additional updates of the model
737 should include human consumption of groundwater resources, identifying areas of higher population
738 density or intensive farming. Future model updates should also account for the interaction of deep rooting
739 species with the surrounding understory species. In particular, shrubs surviving the drought period, which
740 can benefit from the redistribution of groundwater by deep rooted species (Dawson, 1993; Zou et al.,
741 2005).

742 **5 Conclusions**

743 Our results show a highly dominant contribution of water scarcity of the last 30 years (Aridity and
744 Ombrothermic indexes) on the density and suitability of deep-rooted groundwater dependent species in
745 southern Portugal. Therefore, in geographical regions of the world with similar semi-arid climate
746 conditions (Csa according to Köppen-Geigen classification, Peel et al. 2007) and similar physiological
747 responses of the groundwater dependent vegetation (Vicente-Serrano et al., 2013), the use of the aridity
748 and ombrothermic indexes could be used as first approximation to model and map deep rooted
749 phreatophyte species and the evolution of their distribution in response to climate changes. The
750 contribution of groundwater depth was lower than initially expected; however, this might be
751 underestimated due to the poor quality of the piezometric network, especially in the central area of the
752 studied region.

753 The current pressure applied by human consumption of water sources has reinforced the concern on the
754 future of economic activities dependent on groundwater resources. To address this issue, several countries
755 have developed national strategies for the adaptation of water sources for Agriculture and Forests against
756 Climate Change, including Portugal (FAO, 2007). In addition, local drought management as long-term
757 adaptation strategy has been one of the proposals by Iglesias et al. (2007) to reduce the climate change
758 impact on groundwater resources in the Mediterranean. The preservation of Mediterranean agroforestry
759 systems, such as cork oak woodlands and the recently associated *P. pinea* species, is of great importance
760 due to their high socioeconomic value and their supply of valuable ecosystem services (Bugalho et al.,
761 2011). Management policies on the long-term should account for groundwater resources monitoring,
762 accompanied by defensive measures to ensure agroforestry systems sustainability and economical income
763 from these Mediterranean ecosystems are not greatly and irreversibly threatened.

764 Our present study, and novel methodology, provides an important tool to help delineating priority areas of
765 action for species and groundwater management, at regional level, to avoid the decline of productivity
766 and cover density of the agroforestry systems of southern Portugal. This is important to guarantee the
767 sustainability of the economical income for stakeholders linked to the agroforestry sector in that area.
768 Furthermore, mapping vulnerable areas at a small scale (e.g. by hydrological basin), where reliable
769 groundwater depth information is available, should provide further insights for stakeholder to promote
770 local actions to mitigate climate change impact on GDV.

771 Based on the methodology applied in this work, future predictions on GDV suitability, according to the
772 RCP4.5 and RCP8.5 emission scenarios will be shortly introduced, providing guidelines for future
773 management of these ecosystems in the allocation of water resources.

774

775 **6 Acknowledgements**

776

777 The authors acknowledge the E-OBS dataset from the EU-FP6 project ENSEMBLES (<http://ensembles->
778 [eu.metoffice.com](http://ensembles-eu.metoffice.com)) and the data providers in the ECA&D project (<http://www.ecad.eu>). The authors also
779 wish to acknowledge the ASTER GDEM data product, a courtesy of the NASA Land Processes
780 Distributed Active Archive Center (LP DAAC), USGS/Earth Resources Observation and Science (EROS)
781 Center, Sioux Falls, South Dakota, https://lpdaac.usgs.gov/data_access/data_pool. We are grateful to
782 ICNF for sharing inventory database performed in 2010 in Portugal continental. We also thank Cristina
783 Catita, Ana Russo and Patrícia Páscoa for the advice and helpful comments as well as Ana Bastos for the
784 elaboration of the satellite datasets of the vegetation index NDWI and Miguel Nogueira for the insights
785 on model sensitivity analysis. We are very grateful to Eric Font for the useful insights on soil properties. I
786 Gomes Marques and research activities were supported by the Portuguese National Foundation for
787 Science and Technology (FCT) through the PIEZAGRO project (PTDC/AAG-REC/7046/2014). This
788 publication was also supported by FCT- project UID/GEO/50019/2019 – Instituto Dom Luiz. The authors
789 further thank the reviewers and editor for helpful comments and suggestions on an earlier version of the
790 manuscript.

791

792 The authors declare that they have no conflict of interest.

793

794 **References**

- 795 Acácio V. and Holmgreen M.: Pathways for resilience in Mediterranean cork oak land use systems,
796 *Annals of Forest Science*, 71, 5-13, doi: 10.1007/s13595-012- 0197-0, 2014
- 797 Aghakouchak, A., Farahmand, A., Melton, F. S., Teixeira, J., Anderson, M. C., Wardlow, B. D. and Hain
798 C. R.: Remote sensing of drought: Progress, challenges and opportunities. *Rev. Geophys.*, doi:
799 10.1002/2014RG000456, 2015.
- 800 Aksoy, E., Louwagie, G., Gardi, C., Gregor, M., Schröder, C. and Löhnertz, M.: Assessing soil
801 biodiversity potentials in Europe, *Sci. Total Environ.*, 589, 236–249, doi:10.1016/j.scitotenv.2017.02.173,
802 2017.
- 803 Anderson, L. O., Malhi, Y., Aragão, L. E. O. C., Ladle, R., Arai, E., Barbier, N. and Phillips, O.: Remote
804 sensing detection of droughts in Amazonian forest canopies. *New Phytologist*, 187, 733–750, doi:
805 10.1111/j.1469-8137.2010.03355.x, 2010.
- 806 Anselin, L., Ibnu, S. and Youngihn, K.: GeoDa: An Introduction to Spatial Data Analysis, *Geogr. Anal.*,
807 38(1), 5–22, 2006.
- 808 Antunes, C., Chozas, S., West, J., Zunzunegui, M., Barradas, M. C. D., Vieira, S., & Máguas, C.
809 Groundwater drawdown drives ecophysiological adjustments of woody vegetation in a semi-arid coastal
810 ecosystem. *Global Change Biology*, <https://doi.org/10.1111/gcb.14403>, 2018.
- 811 APA: Plano de Gestão da Região Hidrográfica do Tejo: Parte 2 - Caracterização e Diagnóstico da Região
812 Hidrográfica, n.d.
- 813 ARH Alentejo: Plano de Gestão das Bacias Hidrográficas integradas na RH7 - Parte 2, 2012.
- 814 ARH Alentejo: Planos de Gestão das Bacias Hidrográficas integradas na RH6 - Parte 2, 2012.
- 815 Asrar, G. (Ed.): Estimation of plant-canopy attributes from spectral reflectance measurements, *Theory*
816 *and Applications of Optical Remote Sensing*, 252–296, John Wiley, New York, 1989.
- 817 Autoridade Florestal Nacional and Ministério da Agricultura do Desenvolvimento Rural e das Pescas: 5o
818 Inventário Florestal Nacional, 2010.
- 819 Awada T., Radoglou K., Fotelli M. N., Constantinidou H. I. A.: Ecophysiology of seedlings of three
820 Mediterranean pine species in contrasting light regimes, *Tree Physiol.*, 23, 33–41.
- 821 Barata, L. T., Saavedra, A., Cortez, N. and Varennes, A.: Cartografia da espessura efectiva dos solos de
822 Portugal Continental. LEAF/ISA/ULisboa. [online] Available from: [http://epic-webgis-](http://epic-webgis-portugal.isa.utl.pt/)
823 [portugal.isa.utl.pt/](http://epic-webgis-portugal.isa.utl.pt/), 2015.
- 824 Barbero, M., Loisel, R. and Quézel, P.: Biogeography, ecology and history of Mediterranean *Quercus ilex*
825 ecosystems, in *Quercus ilex L. ecosystems: function, dynamics and management*, edited by F. Romane
826 and J. Terradas, 19–34, Springer Netherlands, Dordrecht., 1992.

827 Barbeta, A. and Peñuelas, J.: Increasing carbon discrimination rates and depth of water uptake favor the
828 growth of Mediterranean evergreen trees in the ecotone with temperate deciduous forests, *Glob. Chang.*
829 *Biol.*, 1–15, doi:10.1111/gcb.13770, 2017.

830 Barbeta, A., Mejía-Chang, M., Ogaya, R., Voltas, J., Dawson, T. E. and Peñuelas, J.: The combined
831 effects of a long-term experimental drought and an extreme drought on the use of plant-water sources in a
832 Mediterranean forest, *Glob. Chang. Biol.*, 21(3), 1213–1225, doi:10.1111/gcb.12785, 2015.

833 Barron, O. V., Emelyanova, I., Van Niel, T. G., Pollock, D. and Hodgson, O.G.: Mapping groundwater-
834 dependent ecosystems using remote sensing measures of vegetation and moisture dynamics, *Hydrol.*
835 *Process.*, 28(2), 372–385, doi:10.1002/hyp.9609, 2014.

836 Beguería, S. and Vicente-Serrano, S. M.: SPEI: Calculation of the Standardized Precipitation-
837 Evapotranspiration Index. R package version 1.6., 2013.

838 Bertrand R., Riofrío-Dillon G., Lenoir J., Drapier J., de Ruffray P., Gégout J. C. and Loreau M.:
839 Ecological constraints increase the climatic debt in forests, *Nature Communications*, 7, 12643, doi:
840 10.1038/ncomms12643, 2016.

841 Bivand, R. and Yu, D.: spgwr: Geographically Weighted Regression. [online] Available from:
842 <https://cran.r-project.org/package=spgwr>, 2017.

843 Bivand, R. S., Pebesma, E. J. and Gómez-Rubio, V.: *Applied Spatial Data Analysis with R*, edited by G.
844 P. Robert Gentleman, Kurt Hornik, Springer., 2008.

845 Bourke, L.: Growth trends and water use efficiency of *Pinus pinaster* Ait. in response to historical climate
846 and groundwater trends on the Gngangara Mound, Western Australia. [online] Available from:
847 http://ro.ecu.edu.au/theses_hons/141 (Accessed 29 January 2018), 2004.

848 Bugalho, M. N., Plieninger, T. and Aronson, J.: Open woodlands: a diversity of uses (and overuses), in
849 *Cork oak woodlands on the edge*, edited by J. Aronson, J. S. Pereira, and J. G. Pausas, pp. 33–48, Island
850 Press, Washington DC., 2009.

851 Bugalho, M. N., Caldeira, M. C., Pereira, J. S., Aronson, J. and Pausas, J. G.: Mediterranean cork oak
852 savannas require human use to sustain biodiversity and ecosystem services, *Front. Ecol. Environ.*, 9(5),
853 278–286, doi:10.1890/100084, 2011.

854 Bussotti, F., Ferrini, F., Pollastrini, M. and Fini, A.: The challenge of Mediterranean sclerophyllous
855 vegetation under climate change: From acclimation to adaptation, *Environ. Exp. Bot.*, 103(April), 80–98,
856 doi:10.1016/j.envexpbot.2013.09.013, 2013.

857 Cabon, A., Mouillot, F., Lempereur, M., Ourcival, J.-M., Simioni, G. and Limousin, J.-M.: Thinning
858 increases tree growth by delaying drought-induced growth cessation in a Mediterranean evergreen oak
859 coppice, doi:10.1016/j.foreco.2017.11.030, 2018.

860 Canadell, J., Jackson, R., Ehleringer, J., Mooney, H. A., Sala, O. E. and Schulze, E.-D.: Maximum
861 rooting depth of vegetation types at the global scale, *Oecologia*, 108, 583–595, doi:10.1007/BF00329030,
862 1996.

863 del Castillo, J., Comas, C., Voltas, J. and Ferrio, J. P.: Dynamics of competition over water in a mixed
864 oak-pine Mediterranean forest: Spatio-temporal and physiological components, *For. Ecol. Manage.*, 382,
865 214–224, doi:10.1016/j.foreco.2016.10.025, 2016.

866 Ceccato, P., Gobron, N., Flasse, S., Pinty, B. and Tarantola, S.: Designing a spectral index to estimate
867 vegetation water content from remote sensing data: Part 1. Theoretical approach. *Remote Sens. Environ.*,
868 82, 188 – 197, 2002a

869 Ceccato, P., Flasse, S. and Gregoire, J.: Designing a spectral index to estimate vegetation water content
870 from remote sensing data: Part 2. Validation and applications. *Remote Sens. Environ.*, 82, 198 – 207,
871 2002b

872 Cerasoli S., Silva F.C. and Silva J. M. N.: Temporal dynamics of spectral bioindicators evidence
873 biological and ecological differences among functional types in a cork oak open woodland,
874 *Int. J. Biometeorol.*, 60 (6), 813–825, doi: 10.1007/s00484-015-1075-x, 2016.

875 Chambel, A., Duque, J. and Nascimento, J.: Regional Study of Hard Rock Aquifers in Alentejo, South
876 Portugal: Methodology and Results, in *Groundwater in Fractured Rocks - IAH Selected Paper Series*, pp.
877 73–93, CRC Press., 2007.

878 Chaves M. M., Maroco J. P. and Pereira J.S.: Understanding plant responses to drought — from genes to
879 the whole plant, *Funct Plant Biol*, 30(3), 239 - 264, 2003.

880 Coelho, I. S. and Campos, P.: Mixed Cork Oak-Stone Pine Woodlands in the Alentejo Region of
881 Portugal, in *Cork Oak Woodlands on the Edge - Ecology, Adaptive Management, and Restoration*, edited
882 by J. Aronson, J. S. Pereira, J. Uli, and G. Pausas, pp. 153–159, Island Press, Washington, 2009.

883 Condesso de Melo, M. T., Nascimento, J., Silva, A. C., Mendes, M. P., Buxo, A. and Ribeiro, L.:
884 Desenvolvimento de uma metodologia e preparação do respetivo guia metodológico para a identificação e
885 caracterização, a nível nacional, dos ecossistemas terrestres dependentes das águas subterrâneas
886 (ETDAS). Relatório de projeto realizado para a Agência P., 2015.

887 Condon, L. E. and Maxell, R. M.: Water resources research, *Water Resour. Res.*, 51, 6602–6621,
888 doi:10.1002/2014WR016259, 2015.

889 Costa, A., Madeira, M. and Oliveira, C.: The relationship between cork oak growth patterns and soil,
890 slope and drainage in a cork oak woodland in Southern Portugal, *For. Ecol. Manage.*, 255, 1525–1535,
891 doi:10.1016/j.foreco.2007.11.008, 2008.

892 David, T. S., Ferreira, M. I., Cohen, S., Pereira, J. S. and David, J. S.: Constraints on transpiration from
893 an evergreen oak tree in southern Portugal, *Agric. For. Meteorol.*, 122(3–4), 193–205,
894 doi:10.1016/j.agrformet.2003.09.014, 2004.

895 David, T. S., Henriques, M. O., Kurz-Besson, C., Nunes, J., Valente, F., Vaz, M., Pereira, J. S., Siegwolf,
896 R., Chaves, M. M., Gazarini, L. C. and David, J. S.: Water-use strategies in two co-occurring
897 Mediterranean evergreen oaks: surviving the summer drought., *Tree Physiol.*, 27(6), 793–803,
898 doi:10.1093/treephys/27.6.793, 2007.

899 David, T. S., Pinto, C. A., Nadezhdina, N., Kurz-Besson, C., Henriques, M. O., Quilhó, T., Cermak, J.,
900 Chaves, M. M., Pereira, J. S. and David, J. S.: Root functioning, tree water use and hydraulic
901 redistribution in *Quercus suber* trees: A modeling approach based on root sap flow, *For. Ecol. Manage.*,
902 307, 136–146, doi:10.1016/j.foreco.2013.07.012, 2013.

903 Dawson, T. E.: Hydraulic lift and water use by plants: implications for water balance, performance and
904 plant-plant interactions, *Oecol.*, 95, 565–574, 1993.

905 Dinis, C.O.: Cork oak (*Quercus suber* L.) root system: a structural-functional 3D approach. PhD Thesis,
906 Universidade de Évora (Portugal), 2014

907 Döll, P.: Vulnerability to the impact of climate change on renewable groundwater resources: a global-
908 scale assessment, *Environ. Res. Lett.*, 4(4), 35006–12, doi:10.1088/1748-9326/4/3/035006, 2009.

909 Doody, T. M., Barron, O. V., Dowsley, K., Emelyanova, I., Fawcett, J., Overton, I. C., Pritchard, J. L.,
910 Van Dijk, A. I. J. M. and Warren, G.: Continental mapping of groundwater dependent ecosystems: A
911 methodological framework to integrate diverse data and expert opinion, *J. Hydrol. Reg. Stud.*, 10, 61–81,
912 doi:10.1016/j.ejrh.2017.01.003, 2017.

913 Dresel, P. E., Clark, R., Cheng, X., Reid, M., Terry, A., Fawcett, J. and Cochrane, D.: Mapping
914 Terrestrial Groundwater Dependent Ecosystems: Method Development and Example Output., 2010.

915 Duque-Lazo, J., Navarro-Cerrillo, R. M. and Ruíz-Gómez, F. J.: Assessment of the future stability of cork
916 oak (*Quercus suber* L.) afforestation under climate change scenarios in Southwest Spain, *For. Ecol.*
917 *Manage.*, 409(June 2017), 444–456, doi:10.1016/j.foreco.2017.11.042, 2018.

918 Eamus, D., Froend, R., Loomes, R., Hose, G. and Murray, B.: A functional methodology for determining
919 the groundwater regime needed to maintain the health of groundwater-dependent vegetation, *Aust. J.*
920 *Bot.*, 54(2), 97–114, doi:10.1071/BT05031, 2006.

921 Eamus, D., Zolfaghar, S., Villalobos-Vega, R., Cleverly, J. and Huete, A.: Groundwater-dependent
922 ecosystems: Recent insights from satellite and field-based studies, *Hydrol. Earth Syst. Sci.*, 19(10), 4229–
923 4256, doi:10.5194/hess-19-4229-2015, 2015.

924 Ertürk, A., Ekdal, A., Gürel, M., Karakaya, N., Guzel, C. and Gönenç, E.: Evaluating the impact of
925 climate change on groundwater resources in a small Mediterranean watershed, *Sci. Total Environ.*, 499,
926 437–447, doi:10.1016/j.scitotenv.2014.07.001, 2014.

927 Evaristo, J. and McDonnell, J. J.: Prevalence and magnitude of groundwater use by vegetation: a global
928 stable isotope meta-analysis, *Sci. Rep.*, 7, 44110, doi:10.1038/srep44110, 2017.

- 929 Fan Y., Macho G. M., Jobbágy E. G., Jackson R. B. and Otero-Casal C.: Hydrologic regulation of plant
930 rooting depth. *Proc. Natl Acad. Sci. USA* 114, 10 572–10 577, doi: 10.1073/pnas.1712381114, 2017.
- 931 FAO: Adaptation to climate change in agriculture, forestry and fisheries: Perspective, framework and
932 priorities, Rome, 2007.
- 933 FAO, IIASA, ISRIC, ISS-CAS and JRC: Harmonized World Soil Database (version 1.1), 2009.
- 934 Fernandes, N. P.: Ecosistemas Dependentes de Água Subterrânea no Algarve - Contributo para a sua
935 Identificação e Caracterização, University of Algarve., 2013.
- 936 Ferreira, M. I., Green, S., Conceição, N. and Fernández, J.-E.: Assessing hydraulic redistribution with the
937 compensated average gradient heat-pulse method on rain-fed olive trees, *Plant Soil*, 1–21,
938 doi:10.1007/s11104-018-3585-x, 2018.
- 939 Filella, I. and Peñuelas, J.: Indications of hydraulic lift by *Pinus halepensis* and its effects on the water
940 relations of neighbour shrubs, *Biol. Plant.*, 47(2), 209–214, doi:10.1023/B:BIOP.0000022253.08474.fd,
941 2004.
- 942 Gao, B.C.: NDWI - A normalized difference water index for remote sensing of vegetation liquid water
943 from space. *Remote Sens. Environ.*, 58, 257-266, 1996.
- 944 Gentilesca T., Camarero J. J., Colangelo M., Nolè A. and Ripullone F.: Drought-induced oak decline in
945 the western Mediterranean region: an overview on current evidences, mechanisms and management
946 options to improve forest resilience, *iForest*, 10, 796-806, doi: 10.3832/ifor2317-010, 2017.
- 947 Giorgi, F. and Lionello, P.: Climate change projections for the Mediterranean region, *Glob. Planet.*
948 *Change*, 63(2–3), 90–104, doi:10.1016/j.gloplacha.2007.09.005, 2008.
- 949 Gond, V., Bartholome, E., Ouattara, F., Nonguierma, A. and Bado, L. Surveillance et cartographie des
950 plans d'eau et des zones humides et inondables en regions arides avec l'instrument VEGETATION
951 embarqué sur SPOT-4, *Int. J. Remote Sens*, 25, 987–1004, 2004.
- 952 Gonzalez, P.: Desertification and a shift of forest species in the West African Sahel, *Clim. Res.*, 17, 217–
953 228, 2001.
- 954 Gouveia A. and Freitas H.: Intraspecific competition and water use efficiency in *Quercus suber*: evidence
955 of an optimum tree density?, *Trees*, 22, 521-530, 2008.
- 956 Gouveia C., Trigo R. M., DaCamara C. C.: Drought and Vegetation Stress Monitoring in Portugal using
957 Satellite Data, *Nat. Hazard. Earth Sys.*, 9, 1-11, doi: 10.5194/nhess-9-185-2009, 2009.
- 958 Gouveia C. M., Bastos A., Trigo R. M., DaCamara C. C.: Drought impacts on vegetation in the pre- and
959 post-fire events over Iberian Peninsula, *Nat. Hazard. Earth Sys.*, 12, 3123-3137, doi:10.5194/nhess-12-
960 3123-2012, 2012.
- 961 Grant O. M., Tronina L., Ramalho J. C., Besson C. K., Lobo-do-Vale R., Pereira
962 J. S., Jones H. G. and Chaves M. M.: The impact of drought on leaf physiology of *Quercus suber* L.

963 trees: comparison of an extreme drought event with chronic rainfall reduction,
 964 J. Exp. Bot., 61 (15), 4361–4371, doi: 10.1093/jxb/erq239, 2010.

965 Griffith, D. A. (Ed.): Spatial Autocorrelation, Elsevier Inc, Texas, 2009.

966 Grossiord, C., Sevanto, S., Dawson, T. E., Adams, H. D., Collins, A. D., Dickman, L. T., Newman, B. D.,
 967 Stockton, E. A. and McDowell, N. G.: Warming combined with more extreme precipitation regimes
 968 modifies the water sources used by trees, New Phytol., doi:10.1111/nph.14192, 2016.

969 Gu, Y., J. F. Brown, J. P. Verdin and Wardlow, B.: A five-year analysis of MODIS NDVI and NDWI for
 970 grassland drought assessment over the central Great Plains of the United States, Geophys. Res. Lett., 34,
 971 L06407, doi:10.1029/2006GL029127, 2007.

972 Guisan, A. and Thuiller, W.: Predicting species distribution: Offering more than simple habitat models,
 973 Ecol. Lett., 8(9), 993–1009, doi:10.1111/j.1461-0248.2005.00792.x, 2005.

974 Hagolle, O., Lobo, A., Maisongrande, P., Duchemin, B. and De Pereira, A.: Quality assessment and
 975 improvement of SPOT/VEGETATION level temporally composited products of remotely sensed imagery
 976 by combination of VEGETATION 1 and 2 images, Remote Sens. Environ., 94, 172–186, 2005.

977 Haylock, M. R., Hofstra, N., Klein Tank, A. M. G., Klok, E. J., Jones, P. D. and New, M.: A European
 978 daily high-resolution gridded data set of surface temperature and precipitation for 1950–2006, J. Geophys.
 979 Res. Atmos., 113(20), doi:10.1029/2008JD010201, 2008.

980 Hernández-Santana, V., David, T. S. and Martínez-Fernández, J.: Environmental and plant-based
 981 controls of water use in a Mediterranean oak stand, For. Ecol. Manage., 255, 3707–3715,
 982 doi:10.1016/j.foreco.2008.03.004, 2008.

983 Horton, J. L. and Hart, S. C.: Hydraulic lift: a potentially important ecosystem process, Tree, 13(6), 232–
 984 235, doi:10.1016/j.tree.1998.05.004, 1998.

985 Howard, J. and Merrifield, M.: Mapping groundwater dependent ecosystems in California, PLoS One,
 986 5(6), doi:10.1371/journal.pone.0011249, 2010.

987 Hu, X., Zhang, L., Ye, L., Lin, Y. and Qiu, R.: Locating spatial variation in the association between road
 988 network and forest biomass carbon accumulation, Ecol. Indic., 73, 214–223,
 989 doi:10.1016/j.ecolind.2016.09.042, 2017.

990 Huntsinger, L. and Bartolome, J. W.: Ecological dynamics of *Quercus* dominated woodlands in
 991 California and southern Spain: A state transition model. Vegetation 99–100, 299–305, 1992.

992 ICNF: IFN6 – Áreas dos usos do solo e das espécies florestais de Portugal continental. Resultados
 993 preliminares., Lisboa, 2013.

994 Iglesias, A., Garrote, L., Flores, F. and Moneo, M.: Challenges to manage the risk of water scarcity and
 995 climate change in the Mediterranean, Water Resour. Manag., 21, 775–788, doi:10.1007/s11269-006-
 996 9111-6, 2007.

- 997 Joffre, R., Rambal, S. and Ratte, J. P.: The dehesa system of southern Spain and Portugal as a natural
998 ecosystem mimic, *Agrofor. Syst.*, 45, 57–79, doi:10.1023/a:1006259402496, 1999.
- 999 Kühn, I.: Incorporating spatial autocorrelation may invert observed patterns, *Div. and Dist.*, 13, 66-69,
1000 doi:10.1111/j.1472-4642.2006.00293.x, 2007
- 1001 Kurz-Besson, C., Otieno, D., Lobo Do Vale, R., Siegwolf, R., Schmidt, M., Herd, A., Nogueira, C.,
1002 David, T. S., David, J. S., Tenhunen, J., Pereira, J. S. and Chaves, M.: Hydraulic lift in cork oak trees in a
1003 savannah-type Mediterranean ecosystem and its contribution to the local water balance, *Plant Soil*, 282(1–
1004 2), 361–378, doi:10.1007/s11104-006-0005-4, 2006.
- 1005 Kurz-Besson, C., Lobo-do-Vale, R., Rodrigues, M. L., Almeida, P., Herd, A., Grant, O. M., David, T. S.,
1006 Schmidt, M., Otieno, D., Keenan, T. F., Gouveia, C., Mériaux, C., Chaves, M. M. and Pereira, J. S.: Cork
1007 oak physiological responses to manipulated water availability in a Mediterranean woodland, *Agric. For.*
1008 *Meteorol.*, 184(December 2013), 230–242, doi:10.1016/j.agrformet.2013.10.004, 2014.
- 1009 Kurz-Besson, C., Lousada, J. L., Gaspar, M. J., Correia, I. E., David, T. S., Soares, P. M. M., Cardoso, R.
1010 M., Russo, A., Varino, F., Mériaux, C., Trigo, R. M. and Gouveia, C. M.: Effects of recent minimum
1011 temperature and water deficit increases on *Pinus pinaster* radial growth and wood density in southern
1012 Portugal, *Front. Plant Sci*, 7, doi:10.3389/fpls.2016.01170, 2016.
- 1013 Li, Y., Jiao, Y. and Browder, J. A.: Modeling spatially-varying ecological relationships using
1014 geographically weighted generalized linear model: A simulation study based on longline seabird bycatch,
1015 *Fish. Res.*, 181, 14–24, doi:10.1016/j.fishres.2016.03.024, 2016.
- 1016 Lloret, F., Siscart, D. and Dalmases, C.: Canopy recovery after drought dieback in holm-oak
1017 Mediterranean forests of Catalonia (NE Spain), *Glob. Chang. Biol.*, 10(12), 2092–2099,
1018 doi:10.1111/j.1365-2486.2004.00870.x, 2004.
- 1019 López, B., Sabaté, S., Ruiz, I. and Gracia, C.: Effects of Elevated CO₂ and Decreased Water Availability
1020 on Holm-Oak Seedlings in Controlled Environment Chambers, in *Impacts of Global Change on Tree
1021 Physiology and Forest Ecosystems: Proceedings of the International Conference on Impacts of Global
1022 Change on Tree Physiology and Forest Ecosystems*, held 26--29 November 1996, Wageningen, The
1023 Netherlands, edited by G. M. J. Mohren, K. Kramer, and S. Sabaté, pp. 125–133, Springer Netherlands,
1024 Dordrecht., 1997.
- 1025 Lorenzo-Lacruz, J., Garcia, C. and Morán-Tejeda, E.: Groundwater level responses to precipitation
1026 variability in Mediterranean insular aquifers, *J. Hydrol.*, 552, 516-531, doi:10.1016/j.jhydrol.2017.07.011,
1027 2017.
- 1028 Lowry, C. S. and Loheide, S. P.: Groundwater-dependent vegetation: Quantifying the groundwater
1029 subsidy, *Water Resour. Res.*, 46(6), doi:10.1029/2009WR008874, 2010.
- 1030 Lv, J., Wang, X. S., Zhou, Y., Qian, K., Wan, L., Eamus, D. and Tao, Z.: Groundwater-dependent
1031 distribution of vegetation in Hailiutu River catchment, a semi-arid region in China, *Ecohydrology*, 6(1),
1032 142–149, doi:10.1002/eco.1254, 2013.

1033

1034 Maki, M., Ishiahra, M., Tamura, M.: Estimation of leaf water status to monitor the risk of forest fires by
1035 using remotely sensed data. *Remote Sens. Environ.*, 90, 441–450, 2004.

1036 Mazziotta, A., Heilmann-Clausen, J., Bruun, H. H., Fritz, Ö., Aude, E. and Tøttrup, A. P.: Restoring
1037 hydrology and old-growth structures in a former production forest: Modelling the long-term effects on
1038 biodiversity, *For. Ecol. Manage.*, 381, 125–133, doi:10.1016/j.foreco.2016.09.028, 2016.

1039 Mckee, T. B., Doesken, N. J. and Kleist, J.: The relationship of drought frequency and duration to time
1040 scales, in *AMS 8th Conference on Applied Climatology*, pp. 179–184., 1993.

1041 Mendes, M. P., Ribeiro, L., David, T. S. and Costa, A.: How dependent are cork oak (*Quercus suber* L.)
1042 woodlands on groundwater? A case study in southwestern Portugal, *For. Ecol. Manage.*, 378, 122–130,
1043 doi:10.1016/j.foreco.2016.07.024, 2016.

1044 Middleton, N., Thomas, D. S. G. and Programme., U. N. E.: *World atlas of desertification*, UNEP, 1992.,
1045 London., 1992.

1046 Miller, G. R., Chen, X., Rubin, Y., Ma, S. and Baldocchi, D. D.: Groundwater uptake by woody
1047 vegetation in a semiarid oak savanna, *Water Resour. Res.*, 46(10), doi:10.1029/2009WR008902, 2010.

1048 Ministério da Agricultura do Mar do Ambiente e do Ordenamento do Território: *Estratégia de Adaptação*
1049 *da Agricultura e das Florestas às Alterações Climáticas*, Lisbon, 2013.

1050 Montero, G., Ruiz-Peinado, R., Candela, J. A., Canellas, I., Gutierrez, M., Pavon, J., Alonso, A., Rio, M.
1051 d., Bachiller, A. and Calama, R.: *El pino pinonero (Pinus pinea L.) en Andalucía. Ecología, distribución y*
1052 *selvicultura*, edited by G. Montero, J. A. Candela, and A. Rodriguez, Consejería de Medio Ambiente,
1053 Junta de Andalucía, Sevilla., 2004.

1054 Moran, P. A. P.: Notes on continuous stochastic phenomena, *Biometrika*, 37(1–2), 17–23 [online]
1055 Available from: <http://dx.doi.org/10.1093/biomet/37.1-2.17>, 1950.

1056 Mourato, S., Moreira, M. and Corte-Real, J.: Water resources impact assessment under climate change
1057 scenarios in Mediterranean watersheds, *Water Resour. Manag.*, 29(7), 2377–2391, doi:10.1007/s11269-
1058 015-0947-5, 2015.

1059 Münch, Z. and Conrad, J.: Remote sensing and GIS based determination of groundwater dependent
1060 ecosystems in the Western Cape, South Africa, *Hydrogeol. J.*, 15(1), 19–28, doi:10.1007/s10040-006-
1061 0125-1, 2007.

1062 Nadezhkina, N., Ferreira, M. I., Conceição, N., Pacheco, C. A., Häusler, M. and David, T. S.: Water
1063 uptake and hydraulic redistribution under a seasonal climate: Long-term study in a rainfed olive orchard,
1064 *Ecohydrology*, 8(3), 387–397, doi:10.1002/eco.1545, 2015.

- 1065 Naumburg, E., Mata-Gonzalez, R., Hunter, R., McLendon, T., Martin, D.: Phreatophytic vegetation and
 1066 groundwater fluctuations: a review of current research and application of ecosystem response modelling
 1067 with an emphasis on Great Basin vegetation. *Environ. Manage.*, 35, 726-740, 2005.
- 1068 Neumann, R. B. and Cardon, Z. G.: The magnitude of hydraulic redistribution by plant roots: a review
 1069 and synthesis of empirical and modeling studies, *New Phytol.*, 194(2), 337–352, doi:10.1111/j.1469-
 1070 8137.2012.04088.x, 2012.
- 1071 O’Grady, A. P., Eamus, D., Cook, P. G. and Lamontagne, S.: Groundwater use by riparian vegetation in
 1072 the wet–dry tropics of northern Australia, *Aust. J. Bot.*, 54, 145–154, doi:10.1071/BT04164, 2006.
- 1073 Orellana, F., Verma, P., Loheide, S. P. and Daly, E.: Monitoring and modeling water-vegetation
 1074 interactions in groundwater-dependent ecosystems, *Rev. Geophys.*, 50(3), doi:10.1029/2011RG000383,
 1075 2012.
- 1076 Otieno, D. O., Kurz-Besson, C., Liu, J., Schmidt, M. W. T., Do, R. V. L., David, T. S., Siegwolf, R.,
 1077 Pereira, J. S. and Tenhunen, J. D.: Seasonal variations in soil and plant water status in a *Quercus suber* L.
 1078 stand: Roots as determinants of tree productivity and survival in the Mediterranean-type ecosystem, *Plant*
 1079 *Soil*, 283(1–2), 119–135, doi:10.1007/s11104-004-7539-0, 2006.
- 1080 Paço, T.A., David, T.S., Henriques, M.O.; Pereira, J.S., Valente, F., Banza, J., Pereira, F.L., Pinto, C.,
 1081 David, J.S.: Evapotranspiration from a Mediterranean evergreen oak savannah: The role of trees and
 1082 pasture, *J. Hydrol.*, 369 (1-2), 98–106, doi: 10.1016/j.jhydrol.2009.02.011, 2009.
- 1083 Paulo, J. A., Palma, J. H. N., Gomes, A. A., Faias, S. P., Tomé, J. and Tomé, M.: Predicting site index
 1084 from climate and soil variables for cork oak (*Quercus suber* L.) stands in Portugal, *New For.*, 46, 293–
 1085 307, doi:10.1007/s11056-014-9462-4, 2015.
- 1086 Peel, M.C., Finlayson, B.L. and McMahon, T.A. (2007) Updated World Map of the Köppen-Geiger
 1087 Climate Classification. *Hydrol. Earth Syst. Sci.*, 11, 1633-1644. doi: 10.5194/hess-11-1633-2007.
- 1088 Peñuelas, J. and Filella, I.: Deuterium labelling of roots provides evidence of deep water access and
 1089 hydraulic lift by *Pinus nigra* in a Mediterranean forest of NE Spain, *Environ. Exp. Bot.*, 49(3), 201–208,
 1090 doi:10.1016/S0098-8472(02)00070-9, 2003.
- 1091 Pérez Hoyos, I., Krakauer, N., Khanbilvardi, R. and Armstrong, R.: A Review of advances in the
 1092 identification and characterization of groundwater dependent ecosystems using geospatial technologies,
 1093 *Geosciences*, 6(2), 17, doi:10.3390/geosciences6020017, 2016a.
- 1094 Pérez Hoyos, I., Krakauer, N. and Khanbilvardi, R.: Estimating the probability of vegetation to be
 1095 groundwater dependent based on the evaluation of tree models, *Environments*, 3(2), 9,
 1096 doi:10.3390/environments3020009, 2016b.
- 1097 Pinto C., Nadezhdina N., David J. S., Kurz-Besson C., Caldeira M.C., Henriques M.O., Monteiro F.,
 1098 Pereira J.S., David T.S. Transpiration in *Quercus suber* trees under shallow water table conditions: the
 1099 role of soil and groundwater. *Hydrological processes*, doi: 10.1002/hyp.10097, 2013.

- 1100 Pinto-Correia, T., Ribeiro, N. and Sá-Sousa, P.: Introducing the montado, the cork and holm oak
 1101 agroforestry system of Southern Portugal, *Agrofor. Syst.*, 82(2), 99–104, doi:10.1007/s10457-011-9388-
 1102 1, 2011.
- 1103 QGIS Development Team: QGIS Geographic Information System. Open Source Geospatial Foundation
 1104 Project., 2017.
- 1105 R Development Core Team: R: A language and environment for statistical computing. R Foundation for
 1106 Statistical Computing, Vienna, Austria, 2016.
- 1107 Rivas-Martínez, S., Rivas-Sáenz, S. and Penas-Merino, A.: Worldwide bioclimatic classification system,
 1108 *Glob. Geobot.*, 1(1), 1–638, doi:10.5616/gg110001, 2011.
- 1109 Robinson, T. W.: Phreatophytes, *United States Geol. Surv. Water-Supply Pap.*, (1423), 84, 1958.
- 1110 Rodrigues, C. M., Moreira, M. and Guimarães, R. C.: Apontamentos para as aulas de hidrologia, 2011
- 1111 Sabaté, S., Gracia, C. A. and Sánchez, A.: Likely effects of climate change on growth of *Quercus ilex*,
 1112 *Pinus halepensis*, *Pinus pinaster*, *Pinus sylvestris* and *Fagus sylvatica* forests in the Mediterranean
 1113 region, *For. Ecol. Manage.*, 162(1), 23–37, doi:10.1016/S0378-1127(02)00048-8, 2002.
- 1114 Salinas, M. J., Blanca, G. and Romero, A. T.: Riparian vegetation and water chemistry in a basin under
 1115 semiarid Mediterranean climate, Andarax River, Spain. *Environ. Manage.*, 26(5), 539–552, 2000.
- 1116 Sardans, J. and Peñuelas, J.: Increasing drought decreases phosphorus availability in an evergreen
 1117 Mediterranean forest, *Plant Soil*, 267(1–2), 367–377, doi:10.1007/s11104-005-0172-8, 2004.
- 1118 Sarmento, E. de M. and Dores, V.: The performance of the forestry sector and its relevance for the
 1119 portuguese economy, *Rev. Port. Estud. Reg.*, 34(3), 35–50, 2013.
- 1120 Schenk, H. J. and Jackson, R. B.: Rooting depths, lateral root spreads and belowground aboveground
 1121 allometries of plants in water limited ecosystems, *J. Ecol.*, 480–494, doi:10.1046/j.1365-
 1122 2745.2002.00682.x, 2002.
- 1123 Silva, J. S. and Rego, F. C.: Root to shoot relationships in Mediterranean woody plants from Central
 1124 Portugal, *Biologia*, 59, 109–115, 2004.
- 1125 Singer, M. B., Stella, J. C., Dufour, S., Piégay, H., Wilson, R. J. S. and Johnstone, L.: Contrasting water-
 1126 uptake and growth responses to drought in co-occurring riparian tree species, *Ecohydrology*, 6(3), 402–
 1127 412, doi:10.1002/eco.1283, 2012.
- 1128 Soares, P. M. M., Cardoso, R. M., Ferreira, J. J. and Miranda, P. M. A.: Climate change and the
 1129 Portuguese precipitation: ENSEMBLES regional climate models results, *Clim. Dyn.*, 45(7–8), 1771–
 1130 1787, doi:10.1007/s00382-014-2432-x, 2015.
- 1131 Soares, P. M. M., Cardoso, R. M., Lima, D. C. A. and Miranda, P. M. A.: Future precipitation in Portugal:
 1132 high-resolution projections using WRF model and EURO-CORDEX multi-model ensembles, *Clim Dyn*,
 1133 49, 2503–2530, doi:10.1007/s00382-016-3455-2, 2017.

- 1134 Spinoni, J., Vogt, J. V., Naumann, G., Barbosa, P. and Dosio, A.: Will drought events become more
1135 frequent and severe in Europe?, *Int. J. Climatol.*, 38(4), 1718–1736, doi:10.1002/joc.5291, 2017.
- 1136 Stewart Fotheringham, A., Charlton, M. and Brunsdon, C.: The geography of parameter space: an
1137 investigation of spatial non-stationarity, *Int. J. Geogr. Inf. Syst.*, 10(5), 605–627,
1138 doi:10.1080/02693799608902100, 1996.
- 1139 Stigter, T. Y., Nunes, J. P., Pisani, B., Fakir, Y., Hugman, R., Li, Y., Tomé, S., Ribeiro, L., Samper, J.,
1140 Oliveira, R., Monteiro, J. P., Silva, A., Tavares, P. C. F., Shapouri, M., Cancela da Fonseca, L. and El
1141 Himer, H.: Comparative assessment of climate change and its impacts on three coastal aquifers in the
1142 Mediterranean, *Reg. Environ. Chang.*, 14(S1), 41–56, doi:10.1007/s10113-012-0377-3, 2014.
- 1143 Stone, E. L. and Kalisz, P. J.: On the maximum extent of tree roots, *For. Ecol. Manage.*, 46(1–2), 59–102,
1144 doi:10.1016/0378-1127(91)90245-Q, 1991.
- 1145 Tian, W., Song, J., Li Z., de Wilde, P.: Bootstrap techniques for sensitivity analysis and model selection
1146 in building thermal performance, *Appl. Energ.*, 135, 320-328, doi: 10.1016/j.apenergy.2014.08.110, 2014.
- 1147 Thornthwaite, C. W.: An approach toward a rational classification of climate, *Geogr. Rev.*, 38(1), 55–94,
1148 1948.
- 1149 Valentini, R., Scarascia, G. E. and Ehleringer, J. R.: Hydrogen and carbon isotope ratios of selected
1150 species of a Mediterranean macchia ecosystem, *Funct. Ecol.*, 6(6), 627–631, 1992.
- 1151 Vicente-Serrano, S. M., Beguería, S. and López-Moreno, J. I.: A multiscalar drought index sensitive to
1152 global warming: The standardized precipitation evapotranspiration index, *J. Clim.*, 23(7), 1696–1718,
1153 doi:10.1175/2009JCLI2909.1, 2010.
- 1154 Vicente-Serrano, S. M., Gouveia, C., Camarero, J. J., Begueria, S., Trigo, R., Lopez-Moreno, J. I.,
1155 Azorin-Molina, C., Pasho, E., Lorenzo-Lacruz, J., Revuelto, J., Moran-Tejeda, E. and Sanchez-Lorenzo,
1156 A.: Response of vegetation to drought time-scales across global land biomes, *Proc. Natl. Acad. Sci.*,
1157 110(1), 52–57, doi:10.1073/pnas.1207068110, 2013.
- 1158 Vörösmarty, C. J., Green, P., Salisbury, J. and Lammers, R. B.: Global water resources: Vulnerability
1159 from climate change and population growth, *Science*, 289, 284–288, doi:10.1126/science.289.5477.284,
1160 2000.
- 1161 Waroux, Y. P. and Lambin, E.F.: Monitoring degradation in arid and semi-arid forests and woodlands:
1162 The case of the argan woodlands (Morocco), *Appl Geogr*, 32, 777-786, doi:
1163 10.1016/j.apgeog.2011.08.005, 2012.
- 1164 Xiao R., He X., Zhang Y., Ferreira V. G. and Chang L.: Monitoring groundwater variations from satellite
1165 gravimetry and hydrological models: A comparison with in-situ measurements in the mid-atlantic region
1166 of the United States, *Remote Sensing*, 7 (1), 686–703, doi: 10.3390/rs70100686, 2015.

- 1167 Zomer, R., Trabucco, A., Coe, R., Place, F.: Trees on farm: analysis of global extent and geographical
1168 patterns of agroforestry, ICRAF Working Paper-World Agroforestry Centre, 89, doi:10.5716/WP16263,
1169 2009.
- 1170 Zou, C. B., Barnes, P. W., Archer, S. and Mcmurtry, C. R.: Soil moisture redistribution as a mechanism
1171 of facilitation in savanna tree–shrub clusters, *Ecophysiology*, (145), 32–40, doi:10.1007/s00442-005-
1172 0110-8, 2005.
- 1173
- 1174
- 1175
- 1176
- 1177

1178 **Figure and Table Legends**

1179

1180 Table 1: Environmental variables for the characterization of the suitability of GDV in the study area.

1181 Table 2: Effect of variable removal in the performance of GWR model linking the Kernel density of *Quercus suber*,
1182 *Quercus ilex* and *Pinus pinea* (S_{GDV}) to predictors Aridity Index (A_i); Ombrothermic Index of the summer quarter
1183 and the immediately previous month (O_4); Slope (s); Drainage density (D); Groundwater Depth (W) and Soil type
1184 (S_i). The model with all predictors is highlighted in grey and the final model used in this study is in bold.

1185 Table 3: Comparison of Adjusted R^2 and second-order Akaike Information Criterion (AICc) between the simple
1186 regression and the GWR models.

1187 Table 4: Classification scores for each predictor. A score of 3 was given to highly suitable areas and 1 to less suitable
1188 areas for GDV.

1189 Table A1: Classification scores for soil type predictor.

1190 Table A2: Correlations between predictor variables and principal component axis. The most important predictors for
1191 each axis (when squared correlation is above 0.3) are showed in bold. The cumulative proportion of variance
1192 explained by each principal component axis is shown at the bottom of the table. s is slope; A_i is Aridity Index; O , O_1 ,
1193 O_3 , O_4 are ombrothermic indices of, respectively, the year, the hottest month of the summer quarter, the summer
1194 quarter and the summer quarter and the immediately previous month; SPEIs and SPEIe are, respectively, the number
1195 of months with severe and extreme Standardized Precipitation Evapotranspiration Index; W is Groundwater Depth; D
1196 is the Drainage density; St refers to soil type and T is thickness.

1197

1198 Figure 01: Study area. On the left the location of Alentejo in the Iberian Peninsula; on the right, the elevation
1199 characterization of the study area with the main river courses from Tagus, Sado and Guadiana basins (white lines).
1200 Names of the main rivers are indicated near to their location in the map.

1201 Figure 02: Large well and piezometer data points used for groundwater depth calculation. Squares represent
1202 piezometers data points and triangle represent large well data points.

1203 Figure 03: Map of Kernel Density weighted by cover percentage of *Q. suber*, *Q. ilex* and *P. pinea*. The scale unit
1204 represent the number of occurrences per 10 km search radius ($\sim 314 \text{ km}^2$).

1205 Figure 04: Map of environmental layers used in model fitting. (a) – Aridity Index; (b) – Ombrothermic Index of the
1206 summer quarter and the immediately previous month; (c) – Groundwater Depth; (d) – Drainage density; (e) – Slope.

1207 Figure 05: Spatial distribution of local R^2 from the fitting of the Geographically Weighted Regression.

1208 Figure 06: Spatial distribution of model residuals from the fitting of the Geographically Weighted Regression (a) and
1209 the Simple Linear model (b).

1210 Figure 07: Map of local model coefficients for each variable. (a) – Aridity Index; (b) - Ombrothermic Index of the
1211 summer quarter and the immediately previous month; (c) – Groundwater Depth; (d) – Drainage density and (e) - Slope.

1212 Figure 08: Boxplot of GWR model coefficient values for each predictor (a) and boxplot of the GWR model outputs,
1213 corresponding to GDV's density after each of the predictors was disturbed for the sensitivity analysis (b). A_i stands for
1214 Aridity Index; O_4 for the ombrothermic index of the hottest month of the summer quarter and the immediately previous

1215 month; W for the groundwater depth; D for the drainage density and s for the slope. Error bars represent the 25th and
1216 75th percentile while crosses indicate the 95th percentile.

1217 Figure 09: Suitability map for Groundwater Dependent Vegetation.

1218 Figure 10: Spatial patterns of NDWI anomaly values considering the months of June, July and August of the extremely
1219 dry year of 2005, in reference to the same months of the period 1999-2009, in the Alentejo region. Dark brown colors
1220 (corresponding to extreme negative NDWI anomaly values) indicate the vegetation that experienced the highest loss of
1221 water in leaves in summer 2005 as compared to the reference period 1999-2009, while light brown colors show NDWI
1222 anomaly values very close to the usual vegetation moisture condition of the considered month.

1223 Figure 11: Sensitivity analysis performed on the GWR model by perturbing one of the predictors, while remaining
1224 the rest of the model equation constant. Graphics present the output range of GDV's density when the aridity index
1225 (a), the ombrothermic index (b), the groundwater depth (c), the drainage density (d) or the slope variable (e) was
1226 perturbed; and the maximum possible range combining all predictors (f). The 95th percentile was used for the
1227 maximum value of the color bar for a better statistical representation of the spatial variability.

1228

1229 Figure A1: Boxplot of the main predictors used for the Geographically Weighted Regression model fitting (top) and
1230 the response variable (below), for the total data (left) and for the 5% subsample (right).

1231 Figure A2: Correlation plot between all environmental variables expected to affect the presence of the Groundwater
1232 Dependent Vegetation. O₁, O₃ and O₄ are ombrothermic indices of, respectively, the hottest month of the summer
1233 quarter, the summer quarter and the summer quarter and the immediately previous month; O is the annual
1234 ombrothermic index, SPEI_e and SPEI_s are, respectively, the number of months with extreme and severe Standardized
1235 Precipitation Evapotranspiration Index; A_i is Aridity index; W is groundwater depth; D is the Drainage density; T is
1236 thickness and S_i refers to soil type.

1237 Figure B1 – Predictors maps after score classification. (a) – Aridity Index; (b) – Ombrothermic Index of the summer
1238 quarter and the immediately previous month; (c) – Groundwater Depth; (d) – Drainage density and (e) – Slope.

1239

1240

1241 **Table 1: Environmental variables for the characterization of the suitability of GDV in the study area.**

Variable code	Variable type	Source	Resolution and Spatial extent
s	Slope (%)	This work	0.000256 degrees (25m) raster resolution
S_t	Soil type in the first soil layer	SNIAmb (© Agência Portuguesa do Ambiente, I.P., 2017)	Converted from vectorial to 0.000256 degrees (25m) resolution raster
T	Soil thickness (cm)	EPIC WebGIS Portugal (Barata et al., 2015)	Converted from vectorial to 0.000256 degrees (25m) resolution raster
W	Groundwater Depth (m)	This work	0.000256 degrees (25m) raster resolution
D	Drainage Density	This work	0.000256 degrees (25m) raster resolution
SPEI_s	Number of months with severe SPEI	This work	0.000256 degrees (25m) raster resolution Time coverage 1950-2010
SPEI_e	Number of months with extreme SPEI	This work	0.000256 degrees (25m) raster resolution Time coverage 1950-2010
A_i	Aridity Index	This work	0.000256 degrees (25m) raster resolution Time coverage 1950-2010
O	Annual Ombrothermic Index Annual average (January to December)	This work	0.000256 degrees (25m) raster resolution Time coverage 1950-2010
O₁	Ombrothermic Index of the hottest month of the summer quarter (J, J and A)	This work	0.000256 degrees (25m) raster resolution Time coverage 1950-2010
O₃	Ombrothermic Index of the summer quarter (J, J and A)	This work	0.000256 degrees (25m) raster resolution Time coverage 1950-2010
O₄	Ombrothermic Index of the summer quarter and the immediately previous month (M, J, J and A)	This work	0.000256 degrees (25m) raster resolution Time coverage 1950-2010

1242

1243

1244 **Table 2: Effect of variable removal in the performance of GWR model linking the Kernel density of *Quercus***
 1245 ***suber*, *Quercus ilex* and *Pinus pinea* (SGDV) to predictors Aridity Index (A_i); Ombrothermic Index of the**
 1246 **summer quarter and the immediately previous month (O_4); Slope (s); Drainage density (D); Groundwater**
 1247 **Depth (W); and Soil type (S_t). The model with all predictors is highlighted in grey and the final model used in**
 1248 **this study is in bold.**

Type	Model	Discarded predictor	AICc	Quasi-global R^2
GWR	$S_{GDV} \sim O_4 + A_i + s + D + W + S_t$		27389.74	0.926481
GWR	$S_{GDV} \sim O_4 + s + D + W + S_t$	A_i	28695.14	0.9085754
GWR	$S_{GDV} \sim A_i + s + D + W + S_t$	O_4	28626.88	0.9095033
GWR	$S_{GDV} \sim O_4 + A_i + s + W + S_t$	D	27909.86	0.9184337
GWR	$S_{GDV} \sim O_4 + A_i + D + W + S_t$	s	27429.55	0.924176
GWR	$S_{GDV} \sim O_4 + A_i + s + D + S_t$	W	27742.67	0.9208344
GWR	$S_{GDV} \sim O_4 + A_i + s + D + W$	S_t	18050.76	0.9916192

1249

1250 **Table 3: Comparison of Adjusted R^2 and second-order Akaike Information Criterion (AICc) between the simple**
 1251 **linear regression and the GWR model.**

Model	R^2	AICc	p-value
OLS	0.02	42720	<0.001
GWR	0.99 *	18851	-

1252 *Quasi-global R^2

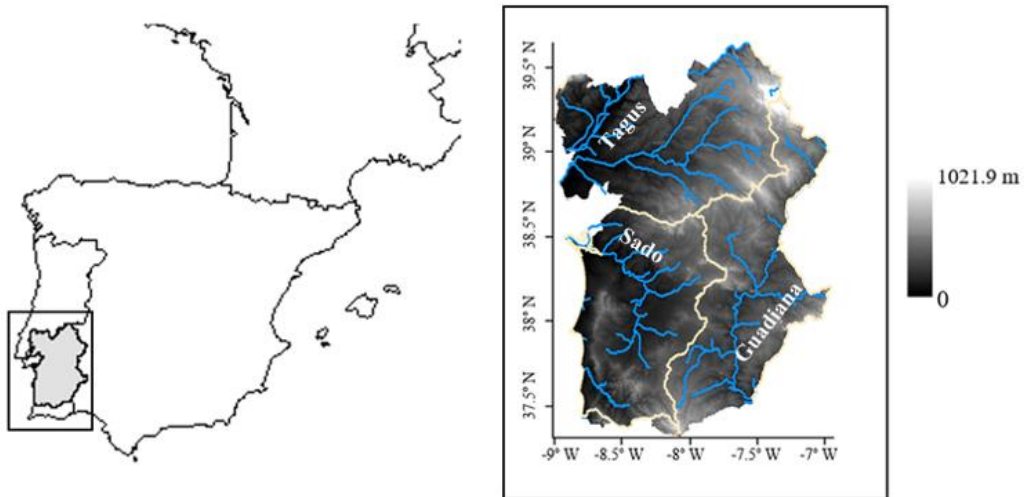
1253

1254 **Table 4: Classification scores for each predictor. A score of 3 was given to highly suitable areas and 1 to less**
 1255 **suitable areas for GDV.**

Predictor	Class	Score
Slope	0%-5%	3
	5%-10%	2
	>10%	1
Groundwater Depth	>15 m	1
	1.5m-15m	3
	≤1.5m	1
Aridity Index	0.6-0.68	3
	0.68-0.75	2
	≥0.75	1
Ombrothermic Index of the summer quarter and the immediately previous month	<0.28	1
	0.28-0.64	2
	≥0.64	3
Drainage Density	≤0.5	3
	>0.5	1

1256

1257

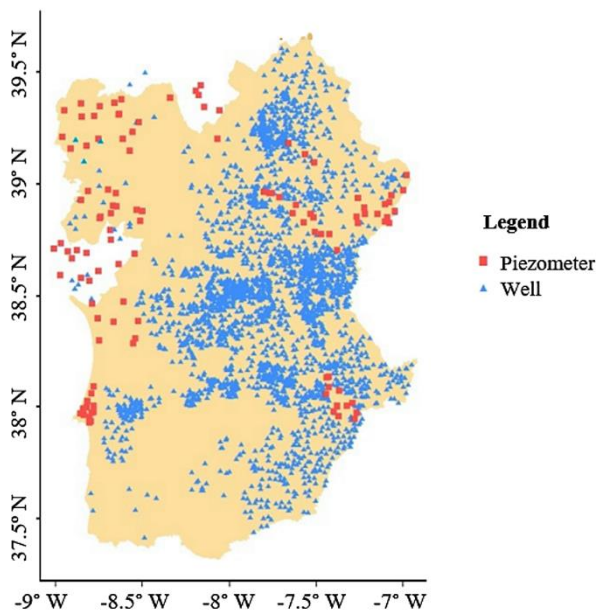


1258

1259 **Figure 01: Study area.** On the left the location of Alentejo in the Iberian Peninsula; on the right, the elevation
1260 characterization of the study area with the main river courses from Tagus, Sado and Guadiana basins (white
1261 lines). Names of the main rivers are indicated near to their location in the map.

1262

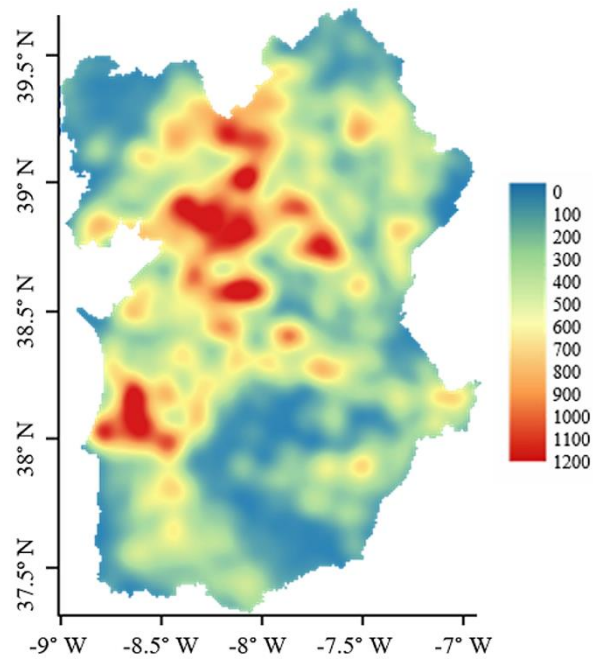
1263



1264

1265 **Figure 02: Large well and piezometer data points used for groundwater depth calculation.** Squares represent
1266 piezometers data points and triangle represent large well data points.

1267

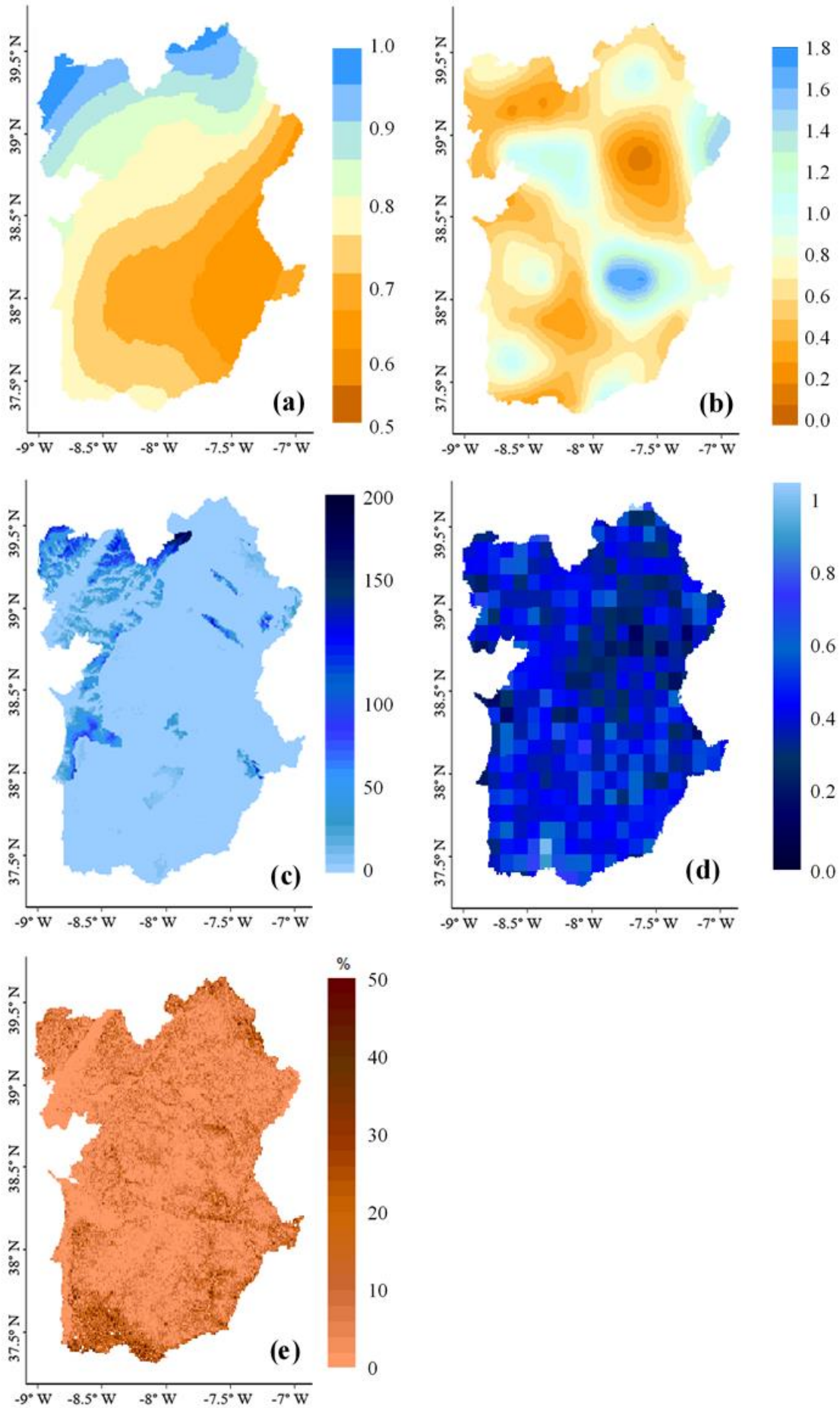


1268

1269 **Figure 03: Map of Kernel Density weighted by cover percentage of *Q. suber*, *Q. ilex* and *P. pinea*. The scale unit**
 1270 **represent the number of occurrences per 10 km search radius (~314 km²).**

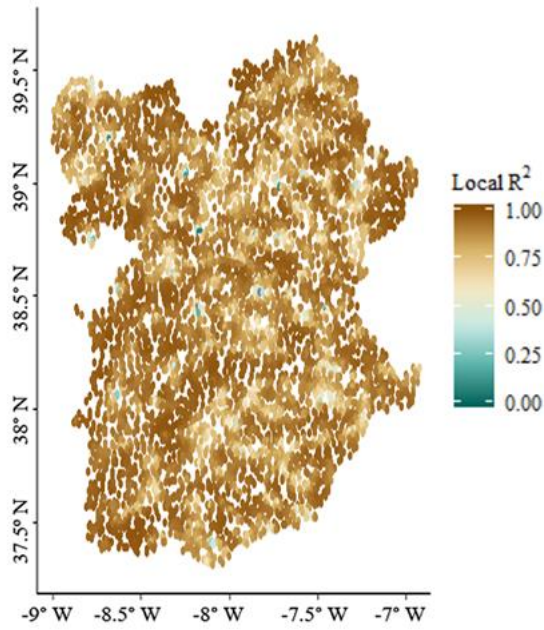
1271

1272



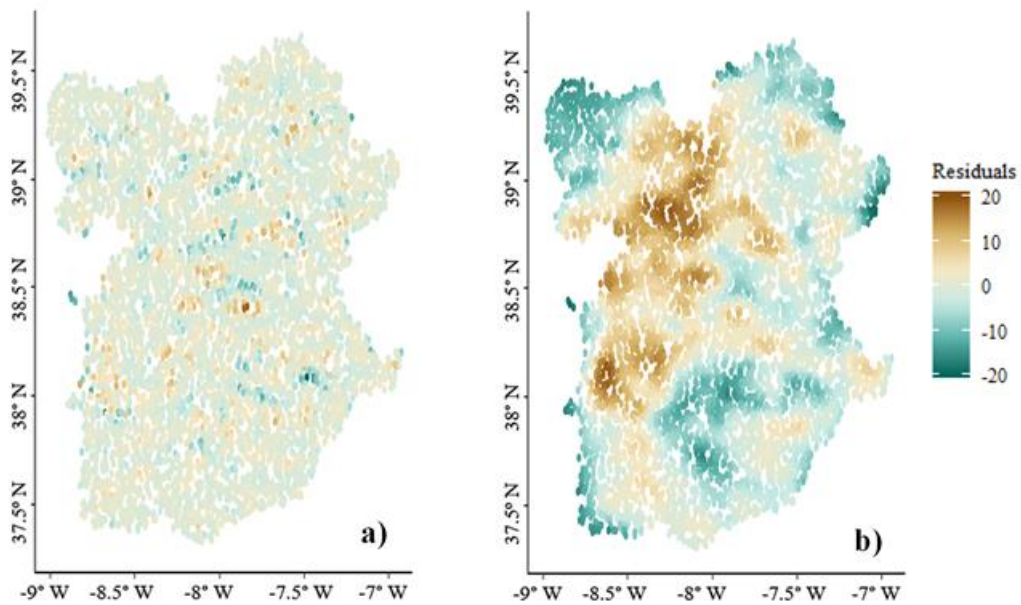
1274 Figure 04: Map of environmental layers used in model fitting. (a) – Aridity Index; (b) – Ombrothermic Index of
1275 the summer quarter and the immediately previous month; (c) – Groundwater Depth; (d) – Drainage density; (e)
1276 – Slope.

1277



1278

1279 Figure 05: Spatial distribution of local R² from the fitting of the Geographically Weighted Regression.



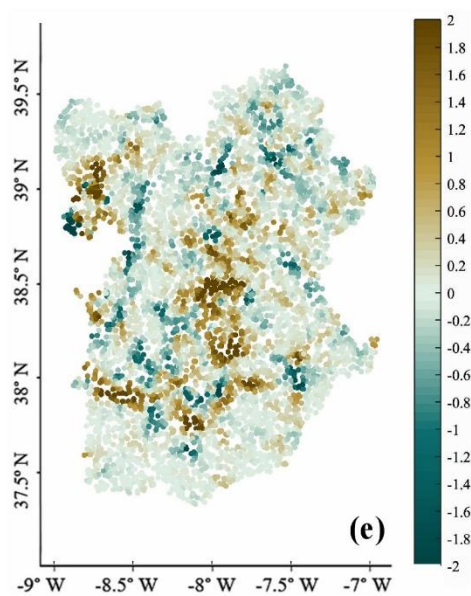
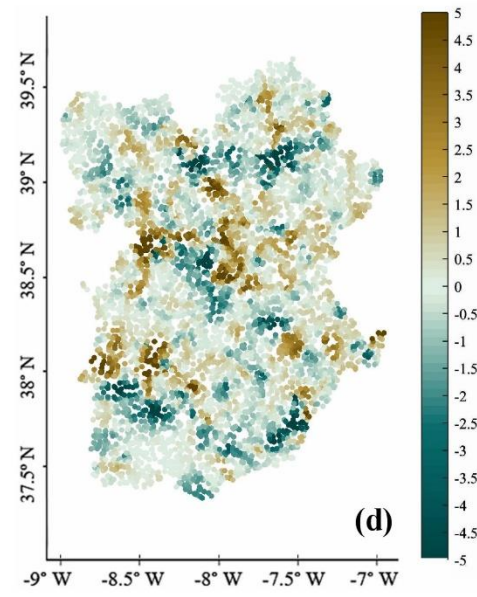
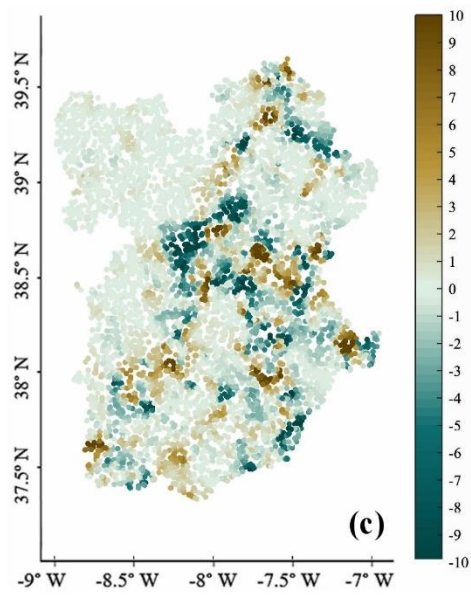
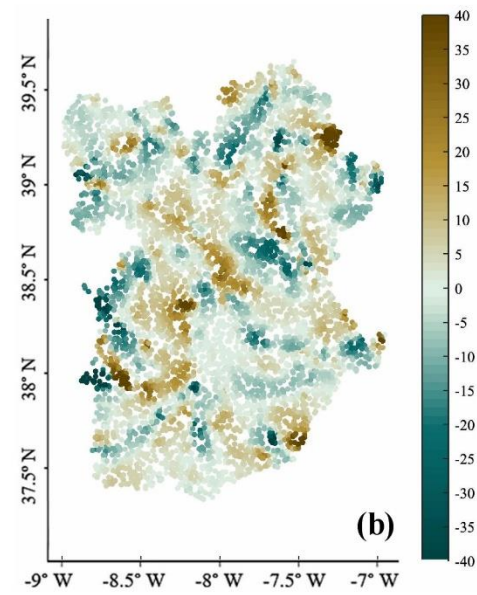
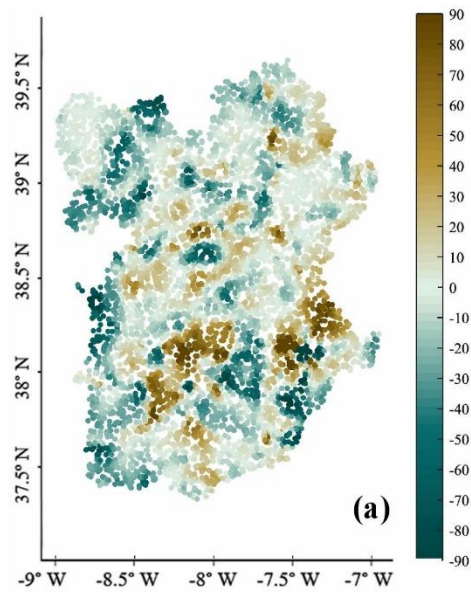
1280

1281 Figure 06: Spatial distribution of model residuals from the fitting of the Geographically Weighted Regression
1282 (a) and Simple Linear model (b).

1283

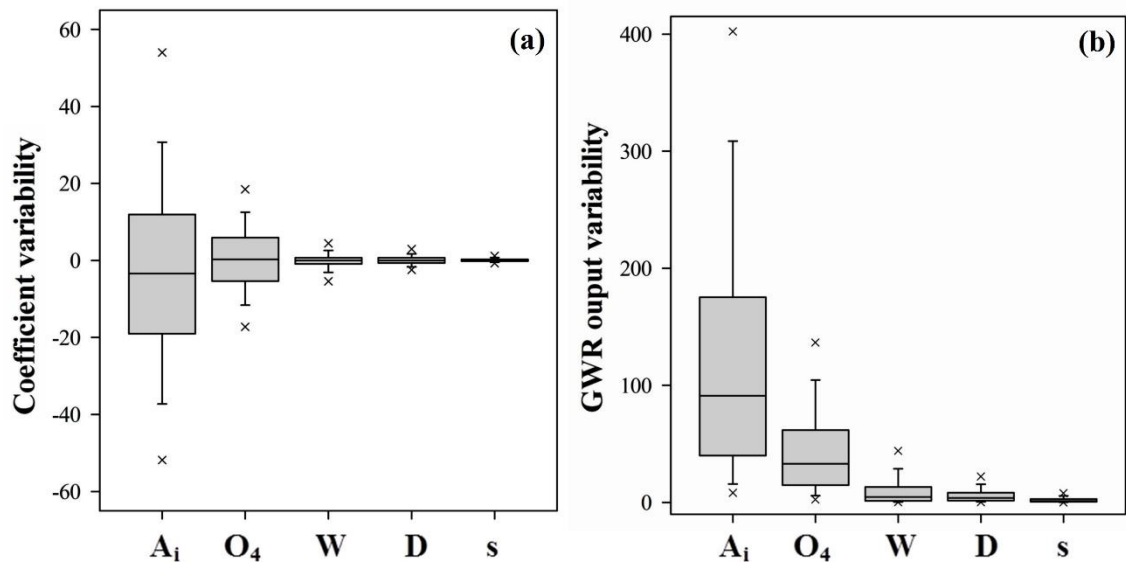
1284

1285



1287 Figure 07: Map of local model coefficients for each variable. (a) – Aridity Index; (b) - Ombrothermic Index of
 1288 the summer quarter and the immediately previous month; (c) – Groundwater Depth; (d) – Drainage density and
 1289 (e) – Slope.

1290

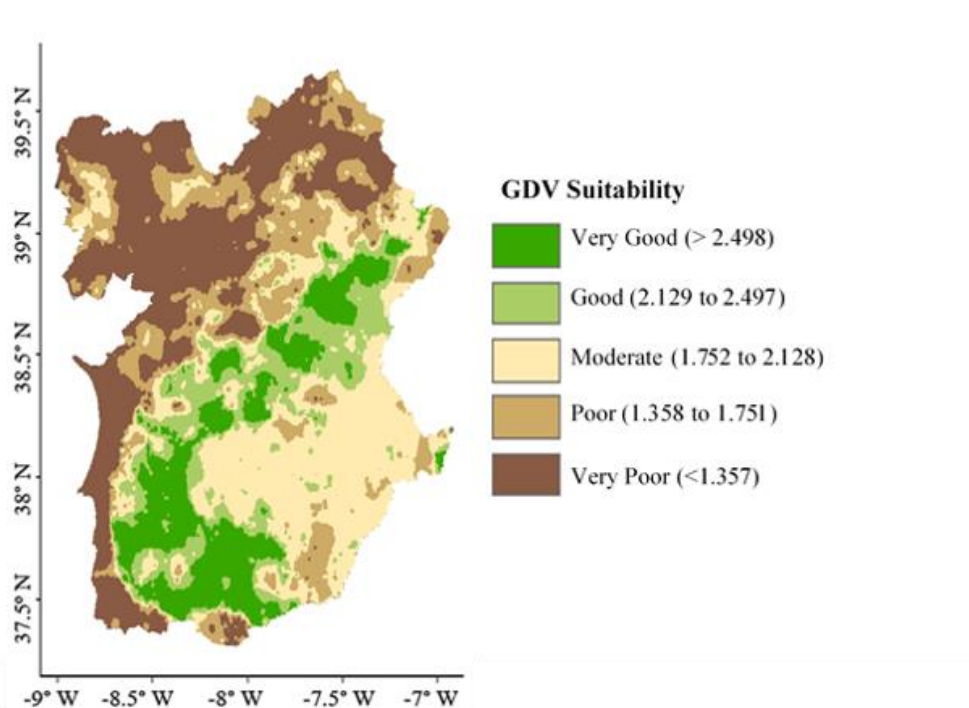


1291

1292 Figure 08: Boxplot of GWR model coefficient values for each predictor (a) and boxplot of the GWR model
 1293 outputs, corresponding to GDV's density after each of the predictors was disturbed for the sensitivity analysis
 1294 (b). Ai stands for Aridity Index; O4 for the ombrothermic index of the hottest month of the summer quarter
 1295 and the immediately previous month; W for the groundwater depth, D for the drainage density and s for the slope.
 1296 Error bars represent the 25th and 75th percentile while crosses indicate the 95th percentile.

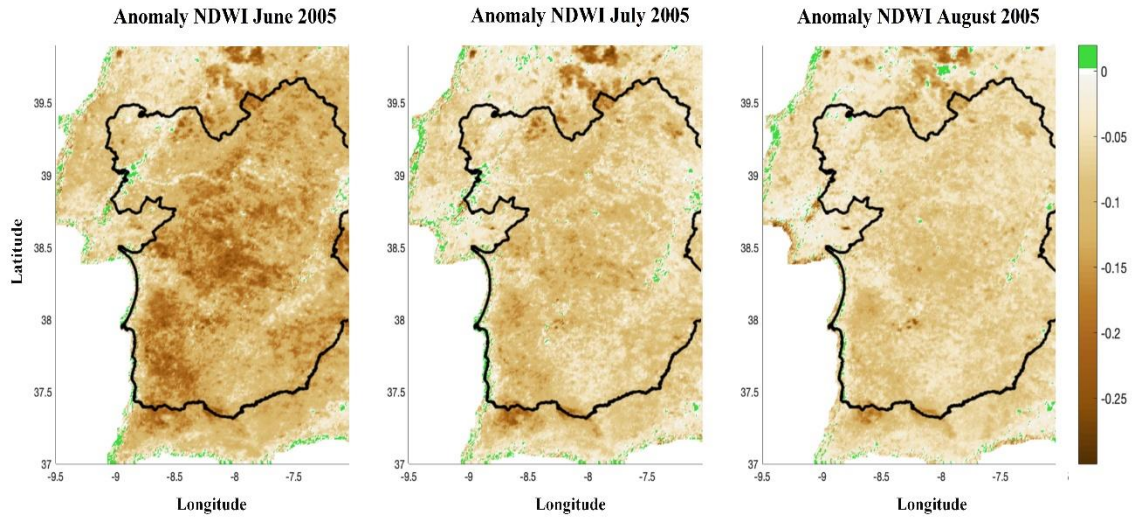
1297

1298



1299

1300 Figure 09: Suitability map for Groundwater Dependent Vegetation.



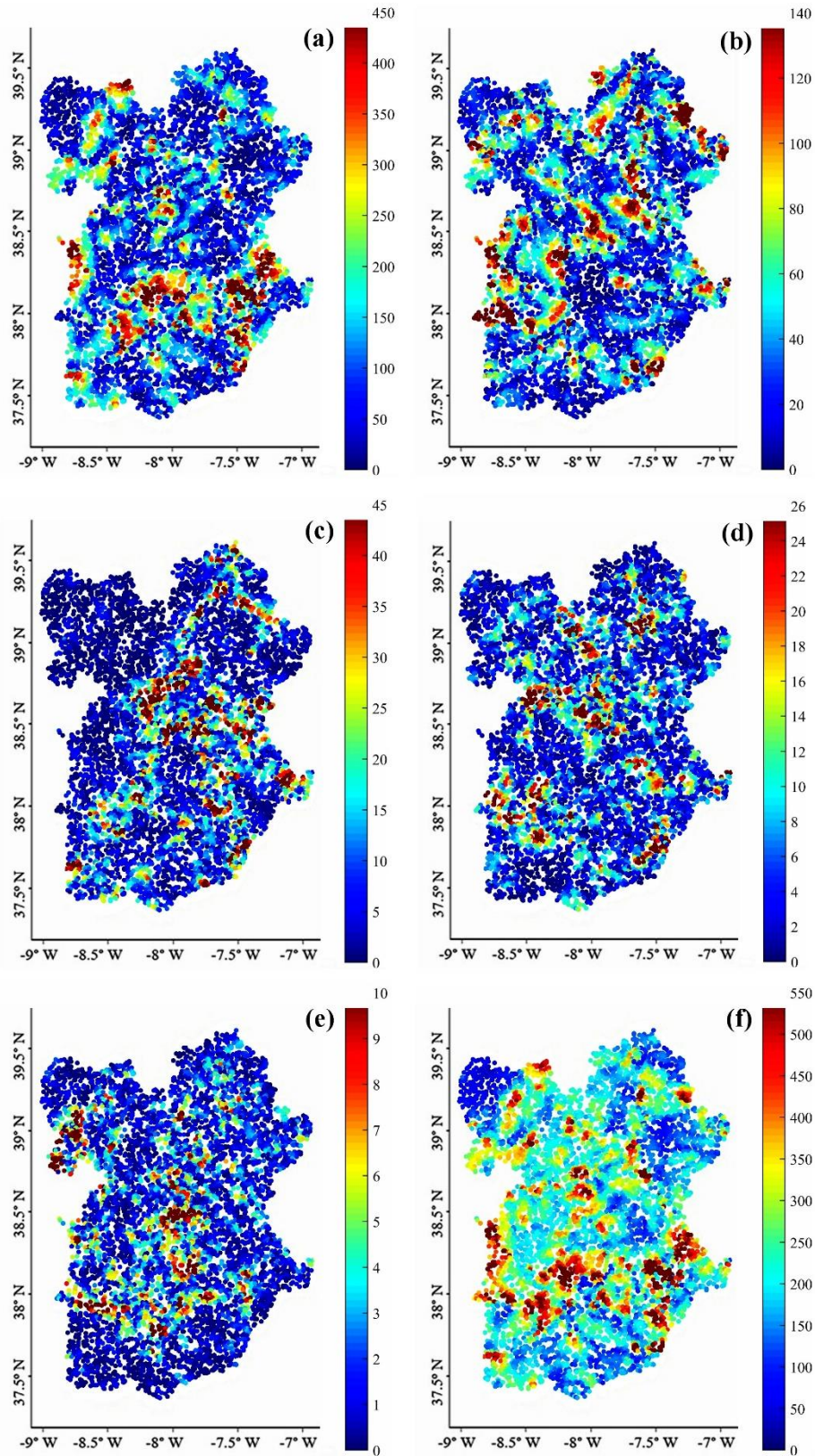
1301

1302 **Figure 10: Spatial patterns of NDWI anomaly values considering the months of June, July and August of the**
 1303 **extremely dry year of 2005, in reference to the same months of the period 1999-2009, in the Alentejo region.**
 1304 **Dark brown colors (corresponding to extreme negative NDWI anomaly values) indicate the vegetation that**
 1305 **experienced the highest loss of water in leaves in summer 2005 as compared to the reference period 1999-2009,**
 1306 **while light brown colors show NDWI anomaly values very close to the usual vegetation moisture condition of**
 1307 **the considered month.**

1308

1309

1310



1311

1312 **Figure 11: Sensitivity analysis performed on the GWR model by perturbing one of the predictors, while**
 1313 **remaining the rest of the model equation constant. Graphics present the output range of GDV's density when**
 1314 **the aridity index (a), the ombrothermic index (b), the groundwater depth (c), the drainage density (d) or the**
 1315 **slope variable (e) was perturbed; and the maximum possible range combining all predictors (f). The 95th**
 1316 **percentile was used for the maximum value of the color bar for a better statistical representation of the spatial**
 1317 **variability.**